Biogeography of the Southern Ocean: environmental factors driving mesoplankton distribution South of Africa

Alexander Vereshchaka, Eteri Musaeva and Anastasiia Lunina

Shirshov Institute of Oceanology, Russian Academy of Sciences, Moscow, Russia

ABSTRACT

Spatial distribution of zooplankton communities depends on numerous factors, especially temperature and salinity conditions (hydrological factor), sampled depth, chlorophyll concentration, and diel cycle. We analyzed and compared the impact of these factors on mesoplankton abundance, biodiversity, quantitative structure based on proportion of taxa and qualitative structure based on presence/absence of taxa in the Southern Ocean. Samples (43 stations, three vertical strata sampled at each station, 163 taxa identified) were collected with a Juday net along the SR02 transect in December 2009. Mesoplankton abundance in discrete vertical layers ranged from 0.2 to 13,743.6 ind. m^{-3}, i.e., five orders of magnitude, maximal and minimal values were recorded in the upper mixed and in the deepest layer, respectively. Within the combined 300-m layer, abundances ranged from 16.0 to 1,455.0 ind. m^{-3}, i.e., two orders of magnitude suggesting that integral samples provide little information about actual variations of mesoplankton abundances. A set of analyses showed that depth was the major driver of mesoplankton distribution (abundance, biodiversity, quantitative structure), hydrological factors influenced two of them (quantitative and qualitative structure), chlorophyll concentration strongly affected only quantitative structure, and diel cycle had an insignificant effect on mesoplankton distribution. Using our current knowledge of the fine structure of the Antarctic Circumpolar Current, we compared effects of four hydrological fronts, i.e., boundaries between different water-masses with distinct environmental characteristics, and eight dynamic jets (narrow yet very intense currents) on mesoplankton distribution. Subtropical, Polar, and Subantarctic Fronts drove quantitative and qualitative structure of mesoplankton assemblages (decreasing in order of influence), while the Southern Boundary affected only qualitative structure. Effects of dynamic jets were insignificant. We suggest that mesoplankton composition is driven by hydrological parameters and further maintained through compartmentalization by fronts. Impact of local eddies and meanders on biodiversity, abundance, qualitative and quantitative structure of mesoplankton is comparable to that of hydrological fronts. Qualitative structure of mesoplankton assemblages mirrors hydrological structure of the Southern Ocean better than quantitative structure and may be recommended for biogeographic analyses of the Southern Ocean. Comparisons with previous reports from the same area retrieved no significant changes in mesoplankton distribution during the period 1992–2009.

INTRODUCTION

Mesoplankton of the Southern Ocean is the key trophic link between phytoplankton microbial production and consumers such as fish, cephalopods, seabirds, and marine mammals (*Atkinson, 1998a*, *1998b*; *Pinkerton & Bradford-Grieve, 2014*). Excretion at depth, egestion, and sinking corpses facilitate the transfer of organic matter to the ocean interior and energetically support benthic communities (*Accornero & Gowing, 2003*; *Steinberg & Landry, 2017*). By grazing on lower trophic levels and forming sinking particles, mesoplankton plays an important role in establishing export carbon regimes in the Southern Ocean (*Halfter et al., 2020*). Mesoplankton is thus a part of the Biological Carbon Pump, which is a critical component of climate regulation (*Lumpkin & Speer, 2007*; *Mayewski et al., 2009*).

Zooplankton distribution is influenced by numerous environmental factors but the impact of some factors is difficult to assess. Temperature, salinity, depth, and diel cycle are the only factors that have been widely studied in relation to plankton assemblages (*Longhurst, 1976*; *Labat et al., 2009*; *Lebourges-Dhaussy et al., 2009*; *Constable et al., 2014*; *Lucas et al., 2014*). There are recent evidences that other environmental factors, such as sea ice and climate indices, may also drive distribution of pteropods (*Thibodeau et al., 2019*) and macroplankton (*Steinberg et al., 2015*), at least near the Western Antarctic Peninsula. As the Southern Ocean is the most remote part of the World Ocean, the impact of environmental factors on plankton assemblages in this region has been studied less than in other oceanic areas. The Discovery Expedition of 1901–1904 (the British National Antarctic Expedition) laid the basis for our knowledge of the biology of the Southern Ocean and resulted in clarification of taxonomic composition, life cycles and distribution of principal plankton groups, such as copepods (*Atkinson, 1991*; *Ommanney, 1936*), chaetognaths (*David, 1955*, *1958*), and various macroplankton taxa (*Mackintosh, 1937*). Later, the Discovery Expedition data were used for assessment of the plankton standing stock in the Southern Ocean by *Foxton (1956)*, who found seasonal variations and a biomass increase near the Polar Front. Since the beginning of the 21st century, several detailed epipelagic studies in the Southern Ocean have shown the dependence of zooplankton characteristics on abiotic gradients associated with hydrological fronts (*Pakhomov et al., 2000*, *2006*, *Pakhomov & Froneman, 2004a*, *2004b*; *Froneman, 2000*; *Ward et al., 2003*; *Jasmine et al., 2009*). Further analysis of the Discovery data showed similar relationships for deeper mesopelagic layers (*Ward et al., 2014*). It is noteworthy that recent studies of plankton distribution in the Southern Ocean have been conducted using continuous plankton recorders (*Labat et al., 2002*, *2009*; *Takahashi et al., 2002*), which provided robust statistics for gross zooplankton characteristics (abundance, biomass), but did not resolve structure of plankton assemblages at the species level. The use of plankton nets followed by the identification of animals is time-consuming, but it is still the only method yielding new detailed representative findings at the species level (*Kulagin, 2010*; *Stupnikova & Vereshchaka, 2013*; *Stupnikova et al., 2018*; *Vedenin et al., 2019*, *2020*).

Historically, two fronts in the Southern Ocean have been defined as the boundary between two zones with distinct water-mass properties: the Subantarctic Front (SAF) and the Polar Front (PF) (*Pakhomov et al., 2000*, *Pakhomov & Froneman, 2004a*, *2004b*; *Froneman, 2000*; *Ward et al., 2003*; *Deacon, 1937*; *Nowlin & Clifford, 1982*). The Antarctic Circumpolar Current (ACC) area also encompasses the Subtropical Front (STF) to the north and the Southern Boundary Front (SB) near Antarctica. In this paper we analyze impact of these four hydrological fronts taking into account that dynamics of the STF and the SB are distinct from the main ACC fronts (*Chapman et al., 2020*).

Now we know that, in addition to classic hydrological fronts, the ACC also includes a system of additional individual jets acting as dynamic fronts and corresponding to sea surface height (SSH) gradients (i.e., intense geostrophic velocities), not sea surface temperature (SST) gradients. Some jets coincide with hydrological fronts, some are lacking sharp gradients of temperature and salinity and thus not synonymous with classic hydrological fronts (*Burkov, 1994*; *Orsi, Whitworth & Nowlin, 1995*; *Tarakanov & Gritsenko, 2014*). Here we note that there is no agreement in the status of the Southern ACC Front (SACCF), which is either recognized as a hydrological front (e.g., *Chapman et al., 2020*) or considered as strictly a dynamic jet (*Tarakanov & Gritsenko, 2014*).

In this paper we tested and hierarchized major environmental factors (hydrological proprieties, depth, diel cycle, chlorophyll concentration) that are responsible for differences between plankton assemblages and further compared the effects individual hydrological fronts and dynamic jets have on the plankton assemblages. With a deeper insight into biogeography of the Southern Ocean, we will better understand important ecosystem services, such as climate regulation and nutrient recycling in such a significant region as the Subantarctic and Polar frontal zones of the ACC area (*Halfter et al., 2020*).

The survey used in this study is based on net samples and aimed to create a detailed analysis of the relationships between environmental factors and the abundance/biodiversity of 129 plankton assemblages. In addition to traditionally studied environmental factors, such as temperature, salinity, hydrological zones (these parameters are highly correlated in the Southern Ocean), depth, and diel cycle, we also tested chlorophyll concentration. Surface chlorophyll-a concentration (*Chl*) recorded by satellite was used as a proxy of biological productivity and can explain characteristics of plankton communities (*Vereshchaka et al., 2016*, *2017*; *Vereshchaka, Lunina & Sutton, 2019*). In this paper, we first compare the impact the environmental factors listed above have on mesoplankton structure in the Southern Ocean.

Another novelty of this paper is the study of the comparative effect of hydrological fronts (boundaries between different water-masses with distinct environmental characteristics) and dynamic jets (narrow yet very intense currents) on the plankton assemblages in the Southern Ocean.

Finally, our survey was made nearly "two decades later" the survey of the same area during the austral summer 1992/1993 (*Pakhomov et al., 2000*). This previous survey was focused on the same plankton group and the same layer 0–300 m and comparison of both
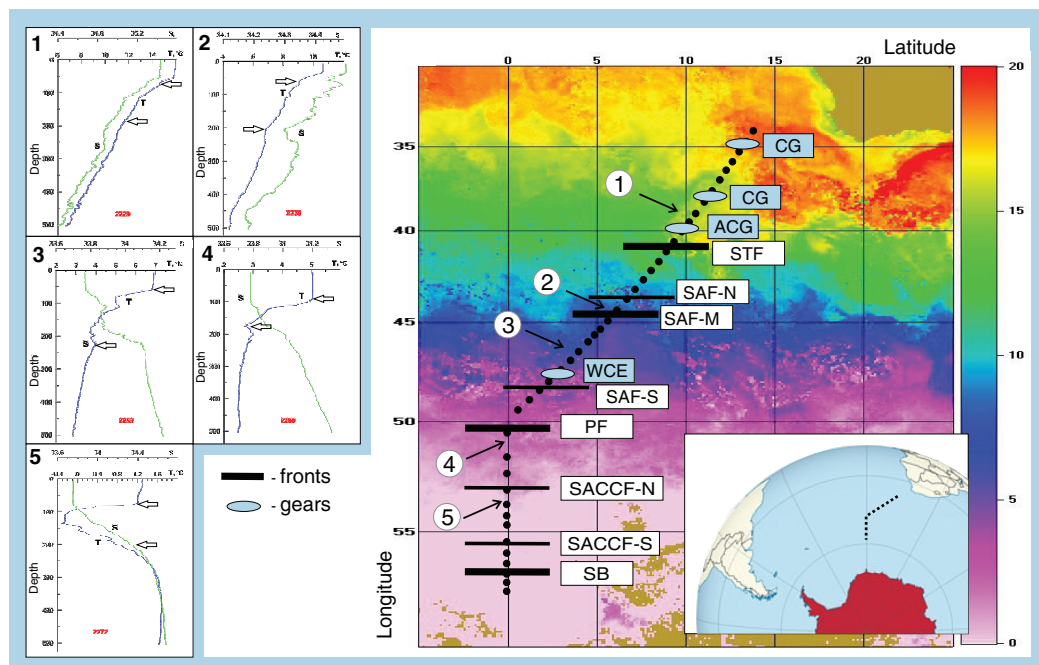
Figure 1 Study area and stations on temperature field (averaged from 30 November to 31 December 2009). Hydrological jet coding: Subtropical Front (STF); Subantarctic Front (SAF), three branches (northern SAF-N, middle SAF-M and southern SAF-S); Polar Front (PF), merged branches; Southern ACC Front (SACCF), two branches (northern SACCF-N and southern SACCF-S); Southern Boundary (SB). Gyre coding: cyclonic gyres (CG), anticyclonic gyres (ACD), warm core eddy (WCE). Characteristic T-S profiles provided for the hydrological zones bounded by jets: arrows indicate vertical boundaries of net hauls and station numbers are in red. Position of fronts and gyres: interpretation after *Tarakanov & Gritsenko (2014)*. Full-size 🖼 DOI: 10.7717/peerj.11411/fig-1

datasets may reveal possible changes (or their absence) in mesoplankton associations in the Southern Ocean.

METHODS

Hydrological setting

The ACC was shown to consist of nine (*Sokolov & Rintoul, 2009*) or even more (*Tarakanov & Gritsenko, 2014*) principal jets or frontal filaments. *Sokolov & Rintoul (2009)* identified the following jets listed from north to south: three branches of the SAF (northern SAF-N, middle SAF-M and southern SAF-S), three branches of the PF (northern PF-N, middle PF-M and southern PF-S), two branches of the SACCF (northern SACCF-N and southern SACCF-S), and a single jet of the SB. Hereafter, we used "fronts" for boundaries between waters masses with sharp hydrological gradients and "jets" for narrow, dynamic fronts. We surveyed the SR02 hydrophysical transect (submeridional, from the South Africa to the Weddell Sea–Fig. 1), where most jets and fronts were well-recognizable, owing to the ACC width and relatively low influence of the bottom relief (*Tarakanov & Gritsenko, 2014*). Since hydrological boundaries are known to vary along longitude and the individual branches can merge and diverge (*Sokolov & Rintoul, 2009*), our sampling was synchronized with a detailed hydrographic survey. Hydrological in

situ data (temperature, salinity, density) were further combined with satellite information and analyzed in detail by *Tarakanov & Gritsenko (2014)*. All ACC structures sensu *Sokolov & Rintoul (2009)* were present, except individual filaments of the PF, which merged and formed a single jet. The zone of the STF was not continuous and consisted of cyclonic and anticyclonic circulations of different genesis, sometimes incorporating Subantarctic waters (*Sokolov & Rintoul, 2009*; *Tarakanov & Gritsenko, 2014*). Using direct measurements (SeaBird 911+ and SBE-21 CTD profilers, a ship-borne Doppler acoustic profiler of the currents SADCP, TRDI Ocean Surveyor, 38 kHz) and the ADT satellite data (the DT-Global-MADT-Upd product from the French agency Collecte Localisation Satellites available at the site http://aviso.oceanobs.com) along the transect, *Tarakanov & Gritsenko (2014)* identified 11 jets, eight of which were identical to dynamic jets sensu *Sokolov & Rintoul (2009)*: a single STF, three branches of the SAF, a single PF, two branches of the SACCF, and the SB. We further analyzed the impact of these eight dynamic jets. *Tarakanov & Gritsenko (2014)* also recorded four hydrological fronts associated with the STF, the SAF-M, the PF, and the SB jets (no gradients in the SACCF jets), which we will further consider as fronts. In addition to fronts and jets, we crossed two cyclonic and one anticyclonic gyres north of the STF (identified and discussed by *Tarakanov & Gritsenko, 2014*) and a single warm core eddy between SAF-M and SAF-S not considered in *Tarakanov & Gritsenko (2014)* but clearly visible in our T-S dataset.

Sample collection and analysis

Samples were taken during the 30th Cruise of the R/V 'Akademik Ioffe' along the SR02 transect (WOCE nomenclature, Fig. 1) between 34.44° S and 56.90° S, from December 5–22, 2009, with intervals of 10–15 h (Fig. 1, Appendix 1). At each station, CTD casts were performed using a SeaBird 911+ profiler prior to biological sampling (see details in *Tarakanov & Gritsenko, 2014*). A total of 43 stations were sampled with a Juday net (0.1 m^2 mouth area, 35 cm diameter, 180 μm mesh size), towed at ~1 m s^{-1}.

We sampled mesoplankton in the active, upper 300 m of the water column (i.e., the whole epipelagic zone and the upper mesopelagic). In order to make hauls vertical, nets were weighted with a 60-kg sinker; the angle of inclination was always ≤ 20° and the spun cable (S_c) was calculated for each haul as: $S_c = D_t \cos(\alpha)^{-1}$, where D_t is target depth and α is angle of inclination. In order to assess the depth factor, we sampled three strata separated by vertical gradients of temperature and salinity at each site. We defined that the Juday net had a filtration coefficient equal to 1 and estimated volume of water filtered (V) as: V (m^3) = 0.1 * L, where L (m) is the difference in the spun cable between the beginning and end point of sampling and 0.1 (m^2) is the mouth area. The net was equipped with the closing device and an operator, which sometimes resulted in insignificant overlapping (<10% of depth ranges) of sampled layers.

The uppermost mixed layer was well-defined and bounded from below by seasonal halo- and thermoclines; two deeper layers were separated from each other by maximal gradients of temperature and salinity between the thermocline and 300 m depth. Actual sampling depths ranged along the transect; the upper and intermediate layers usually represented the epipelagic zone, while the deep layer occurred mainly in the upper

mesopelagic (Fig. 1, Appendix 1). On average, in the upper, intermediate, and deep layers we filtered 6.20 ± 1.93 m³, 12. 31 ± 2.76 m³, and 11.76 ± 2.54 m³, respectively (Mean ± SD).

Samples were preserved in 4% seawater/buffered formaldehyde solution (250–500 ml each sample) and identified to the lowest possible taxonomical level using a stereomicroscope. In order to avoid bias linked to unrepresentative sampling of larger organisms (jellyfishes, salps, and euphausiids over 10 mm total length), we excluded these groups from analyses. Most taxa were counted in the whole sample; abundant taxa, such as *Oithona, Oncaea*, nauplii, and small copepodites were counted in the aliquots, which were sub-sampled with Stempel pipettes. In the aliquots (1/10–1/2 of the total sample), a minimum 100 individuals of each taxon were counted.

Mesoplankton abundance and diversity indices used

We analyzed quantitative (QNT) and qualitative (QUAL) structure of plankton assemblages using quantitative and qualitative Bray–Curtis indices, respectively. The quantitative Bray–Curtis was based on an untransformed dataset and described taxa proportion in the assemblages and quantitative mesoplankton structure. The qualitative index was based on a presence-absence transformation of the dataset and sensitive to rare species and better mirrored all recorded taxa. We used qualitative indices because tests based on original abundance values are often over-dominated by a small number of highly abundant species and therefore fail to reflect overall community composition (*Clarke & Warwick, 2001*). This argument may be particularly true for our dataset: the survey was made in December, when most seasonal migrants ascended into the upper layer and a complete set of species was present in plankton assemblages (*Hardy & Gunther, 1935*; *Mackintosh, 1934*; *Voronina, 1984*). However, the transect crossed hydrological zones with different biological seasons, and abundances of some taxa could be underestimated in higher latitudes, where populations still partially occurred below 300 m depth. Indeed, recent use of qualitative approach in the analyses of plankton communities of the Drake Passage resulted in a more comprehensible outcome than the use of quantitative indices (*Vedenin et al., 2019*).

Biodiversity was estimated using the taxa number, and Shannon (*H*) and Dominance (*D*) indices. *H* (entropy) varies from 0 for communities with only a single taxon to high values for communities with many taxa, each with few individuals. *D* ranges from 0 (all taxa are equally represented) to 1 (one taxon dominates the community completely). Both indices were calculated as

$$H = -\sum_{i=1}^{R} p_i \ln p_i$$

$$D = \sum_{i=1}^{R} (p_i)^2$$

where p_i is the proportion of individuals belonging to the i-th species in the dataset with R taxa.

Determining the impact of environmental factors on mesoplankton abundance and biodiversity

Canonical Correspondence Analyses (CCAs: *Ter Braak, 1986*; *Legendre & Legendre, 1998*) were conducted in order to compare the impact of major environmental factors on plankton communities. We scored four environmental factors and divided each factor by ordinals:

- Hydrological zones/temperature/salinity: For each station, we collected information about temperature and salinity at the surface and at a depth of 300 m (deepest sampled depth). In addition, we calculated average temperature and salinity for each sampled vertical layers on the basis of temperature profiles (Appendix 1). In order to assess and compare effects of hydrological fronts and jets, we completed two analyses: we first divided the transect into five zones bounded by four hydrological fronts (Analysis 1) and then into nine zones bounded by eight jets (Analysis 2–Table 1). If a station was located exactly on a jet or on a front boundary, it was referred to both neighboring zones. In our dataset, temperature and salinity values and hydrological zones were highly correlated. In order to avoid collinearity in the CCAs, we chose hydrological zones and considered them as ordinals: 1–5 in Analysis 1 and 1–9 in Analysis 2. Hereafter, the terms "hydrological zone" will refer to a region bounded by two fronts or jets, and "hydrological factor" will refer to temperature and salinity, keeping in mind that either of these variables (or likely both) contribute to the effect of this factor.
- Depth: Sampled strata were coded as ordinals: 1 (upper mixed layer), 2 (intermediate layer), and 3 (deep layer).
- Diel cycle: Conditions were expressed by three ordinals: 1 (night), 2 (dusk), and 3 (day). Dusk was defined as the time period between one hour before and one hour after sunrise or sunset, local time.
- Chlorophyll concentration (*Chl*): The data were retrieved from satellite imaging and were used as a proxy of biological productivity. The values were obtained from Aqua MODIS scanner (level 3, 4-km resolution, https://oceancolor.gsfc.nasa.gov/) and averaged over the month of the survey (December 2009) and over a 1° (latitude) × 5° (longitude) rectangle with the sampling site in the center. *Chl* values were further divided into six ranges and scored as ordinals: 1 (0.20–0.25 mg m^{-3}), 2 (0.25–0.30 mg m^{-3}), 3 (0.30–0.35 mg m^{-3}), 4 (0.35–0.40 mg m^{-3}), 5 (0.40–0.45 mg m^{-3}), and 6 (0.45–0.50 mg m^{-3}).

All four factors were not correlated (pairwise correlations were checked).

We used pairwise two-way analyses of similarities (ANOSIM) to determine the difference between samples grouped by hydrological zones, depth, diel cycle, and *Chl* ranges. We also used an ANOSIM test for a pairwise comparison between stations bounded by hydrological fronts (Analysis 1) and dynamic jets (Analysis 2).

Table 1 List of dominant taxa (>0.1% contribution to the total abundances).

Taxa	Contribution, %
1. *Oithona similis*	49.20
2. Calanoida copepodites indet.	11.86
3. Euphausiidae nauplii	4.91
4. *Ctenocalanus citer*	4.89
5. Foraminifera	4.62
6. Ova (copepoda)	3.06
7. *Microcalanus pusillus*	2.82
8. Appendicularia	2.70
9. Radiolaria	2.04
10. *Clausocalanus brevipes*	1.36
11. *Triconia antarctica* ♂	1.29
12. *Clausocalanus pergens*	1.10
13. *Paracalanus parvus parvus*	0.81
14. *Oncaea* sp.	0.67
15. *Pleuromamma gracilis*	0.65
16. Ostracoda	0.56
17. *Metridia lucens lucens*	0.49
18. Chaetognatha	0.45
19. *Acartia longiremis*	0.43
20. Copepoda nauplii	0.43
21. *Calanus simillimus*	0.42
22. *Calocalanus contractus*	0.39
23. Pteropoda	0.39
24. *Scolecithricella minor*	0.35
25. *Oithona plumifera*	0.34
26. *Ctenocalanus vanus*	0.31
27. *Calocalanus styliremis*	0.30
28. *Calanus propinquus*	0.29
29. *Euchaeta marina*	0.25
30. *Triconia antarctica* ♀	0.23
31. *Onychocorycaeus giesbrechti*	0.19
32. Euphausiacea calyptopis	0.19
33. Salpidae	0.18
34. *Clausocalanus laticeps*	0.15
35. Euphausiacea furcilia	0.14
36. *Rhincalanus gigas*	0.11

We used traditional plots of abundance and diversity in the depth-latitude coordinates to visualize the impact of depth and hydrological zones. The plots were made using the SURFER package (v. 11.0.642, grid method: kriging, smoothing: low) in order to show trends in distribution.

Vereshchaka et al. (2021), *PeerJ*, DOI 10.7717/peerj.11411

8/35

For a more in depth analysis of the impact of hydrological boundaries, we assessed the discontinuities of plankton communities along the transect. We used a number of unique taxa (NUT), which were present at a given station and absent at both neighboring stations. NUT values were smoothed using the Gaussian, "nine points" algorithm.

The Bray–Curtis matrices were also analyzed using hierarchical clustering, the Unweighted Pair-Group Method (UPGMA). Results were verified by Similarity Profile Analysis (SIMPROF) to distinguish different groups with significant differences in variables (*Clarke & Warwick, 2001*).

Statistics were performed using Primer v6, Past 3, Surfer 15 and Microsoft Excel 2010 software (*Clarke & Warwick, 2001*; *Hammer, Harper & Ryan, 2008*). We accepted a significance level of $p = 0.05$.

RESULTS

Composition of zooplankton assemblages and distribution of dominant taxa

We identified 163 taxa, predominately copepods (dominant taxa listed in Table 1, full list in Appendix 2). *Oithona similis* composed nearly half of the mesoplankton abundance and was followed by four other taxa, each contributing >4% to the total abundance: unidentified young calanoid copepodites, euphausiid nauplii, *Ctenocalanus citer*, and Foraminifera. These five taxa accounted for over 75.49% of the total mesoplankton abundance.

Distribution of all three biodiversity indices suggested the highest biodiversity north of 37° S (Figs. 2C–2E), i.e., in the core waters of the Agulhas Current (Figs. 2A, 2B). Within the ACC, biodiversity indices did not show visible horizontal trends along the transect, except a plankton-depleted gap between 47° and 50° S (Figs. 2C–2E). Highest biodiversity was recorded in the deep layer (maximal H and minimal D values), i.e., evenness of planktonic assemblages grew with depth (Figs. 2C–2E).

High abundances of mesoplankton, including all five dominant taxa, were generally observed between the STF and the SB, with a notable gap between 47° and 50° S (Figs. 3A–3F). Increased abundances of the total mesoplankton, *O. similis*, and calanoid copepodites were locally observed north of the STF and were associated with the subtropical anticyclonic gyre (Figs. 3A–3C). In contrast to biodiversity indices, highest abundance of dominant taxa was recorded mostly in the upper mixed layer.

No notable changes in biodiversity indices, abundance of dominant taxa and total mesoplankton abundance were visibly associated with individual hydrological fronts or jets.

Comparative impact of major environmental factors on mesoplankton abundance and biodiversity

Multivariate CCAs using a quantitative approach (QNT-structure of mesoplankton) showed similar results for Analysis 1 (stations bounded by hydrological fronts, Fig. 4A) and Analysis 2 (stations bounded by jets, Fig. 4C). Two first major factors (thereafter named F1, F2) explained together almost 92% of the variance of the dataset and they were
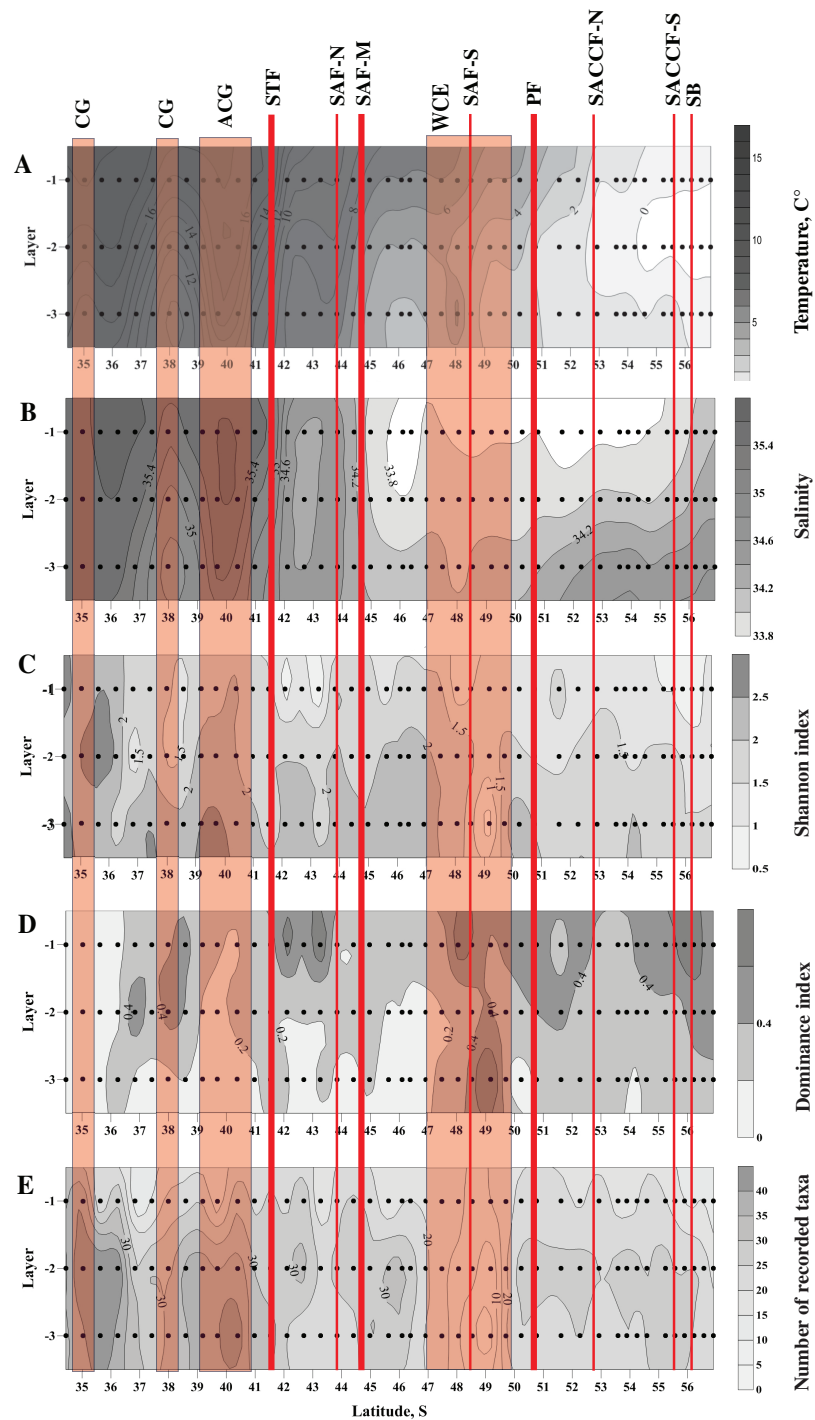
Figure 2 Distribution of temperature (C°) and salinity averaged for sampled layers (A and B, respectively), Shannon and Dominance biodiversity indices (C and D, respectively), and number of recorded taxa (E); scales presented on the right of the plots. Dots indicate the position of the samples. Vertical layer coding is as follows: upper mixed layer (1), intermediate layer (2), deep sampled layer (3). Hydrological jet coding (vertical red lines): Subtropical Front (STF); Subantarctic Front (SAF), three branches (northern SAF-N, middle SAF-M and southern SAF-S); Polar Front (PF), merged

subequally linked to hydrological zone and depth and to a lesser extent with *Chl*. Diel cycle factor was insignificant.

CCAs using a qualitative approach (QUAL-structure of mesoplankton) also showed similar results for Analysis 1 and Analysis 2 (Figs. 4B and 4D), but these results were significantly different from those obtained with the quantitative approach. Factor F1 explained ~67% of variance and was strongly linked only to hydrological zone. The three other factors were subequal and less significant.

Pairwise two-way ANOSIM tests confirmed results of CCAs and revealed constant statistically significant differences between assemblages bounded by hydrological zone, depth, and *Chl* (Table 2). Both quantitative and qualitative approaches resulted in a robust difference provided by these three factors in all combinations. Diel cycle did not provide a statistically significant separation in any of the pairwise combinations, which is in agreement with the results of CCAs. In both two-way ANOSIM tests and CCAs the results are the same for hydrological zones delimited by fronts or jets. The specific difference between fronts and jets in shaping the distribution of zooplankton assemblages is further explored in the following section.

Comparative impact of hydrological fronts and dynamic jets on mesoplankton abundance and biodiversity

Discontinuities of assemblages assessed through the NUT (number of the unique taxa) index showed a general southward decrease along the transect from maximal values at two northernmost stations and minimal values at the southernmost station. Two remarkable maxima were, however, observed along the transect with different position in the upper mixed layer and underlying layers. In the upper layer, NUT maxima were associated with two hydrological fronts (the STF and the PF: green line in Fig. 5), while in deeper layers NUT maxima were recorded northernmore: within an anticyclonic gyre of the Agulhas Current near 40° S and the warm core eddy at ~40° S (blue and red lines in Fig. 5). There was no visible association of NUT peaks with the dynamic jets.

The ANOSIM tests (Table 3) confirmed the strong separating effect of the three hydrological fronts (STF, SAF-M, PF) and an insignificant effect of the dynamic jets. When we divided plankton assemblages into five groups bounded by hydrological fronts and used the qualitative approach (study of QUAL-stricture), all groups were significantly different from each other, except the fifth group bounded by the SB (ANOSIM tests in Table 3 and MDS scaling in Appendix 3). This effect was observed for each individual layer and for the whole 300-m layer with the exception of a boundary between the second and third groups in the deep layer. The quantitative approach (study of QNT-structure-Appendix 4) resulted in fewer statistically significant boundaries: the STF (all layers), the PF (intermediate and deep layers), and the SB (upper layer).

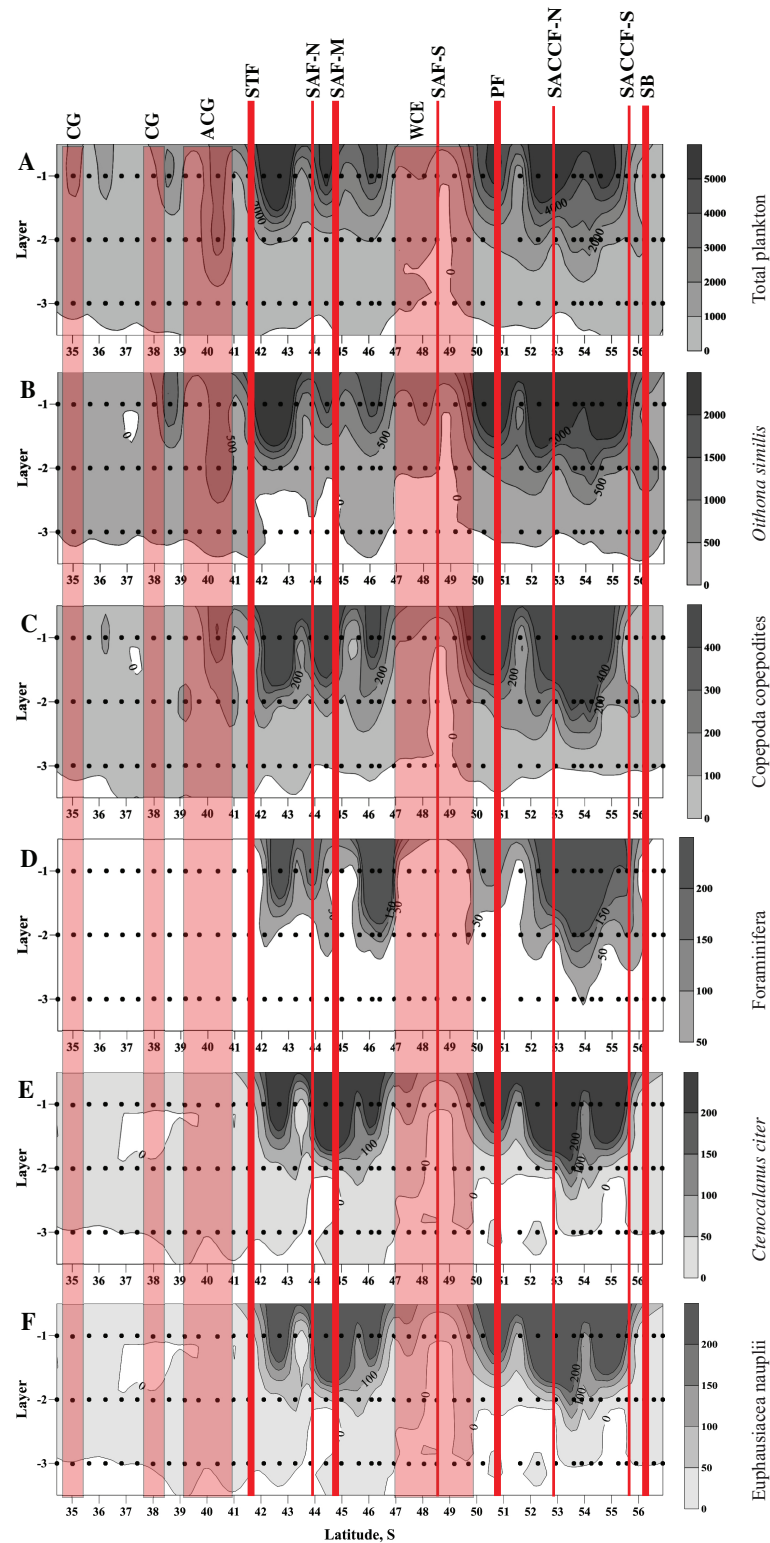**Figure 3 Distribution of total plankton abundance (A), abundances of *Oithona similis* (B), Copepoda copepodites (C), Foraminifera (D), *Ctenocalanus citer* (E), and Euphausiacea nauplii (F).** Scales presented on the right of the plots (abundance: ind. m^{-3}). Dots indicate position of samples. Vertical layer coding: upper mixed layer (1), intermediate layer (2), deep layer (3). Hydrological jet

Figure 3 (continued)
coding (vertical red lines): Subtropical Front (STF); Subantarctic Front (SAF), three branches (northern SAF-N, middle SAF-M and southern SAF-S); Polar Front (PF), merged branches; Southern ACC Front (SACCF), two branches (northern SACCF-N and southern SACCF-S); Southern Boundary (SB). Gyre coding (vertical opaque red strips, interpretation after *Tarakanov & Gritsenko (2014)*): cyclonic gyre (CG) and anticyclonic gyre (ACG). Position of fronts and gyres: interpretation after *Tarakanov & Gritsenko (2014)*. SURFER 11.0.642, grid method: kriging, smoothing: low.
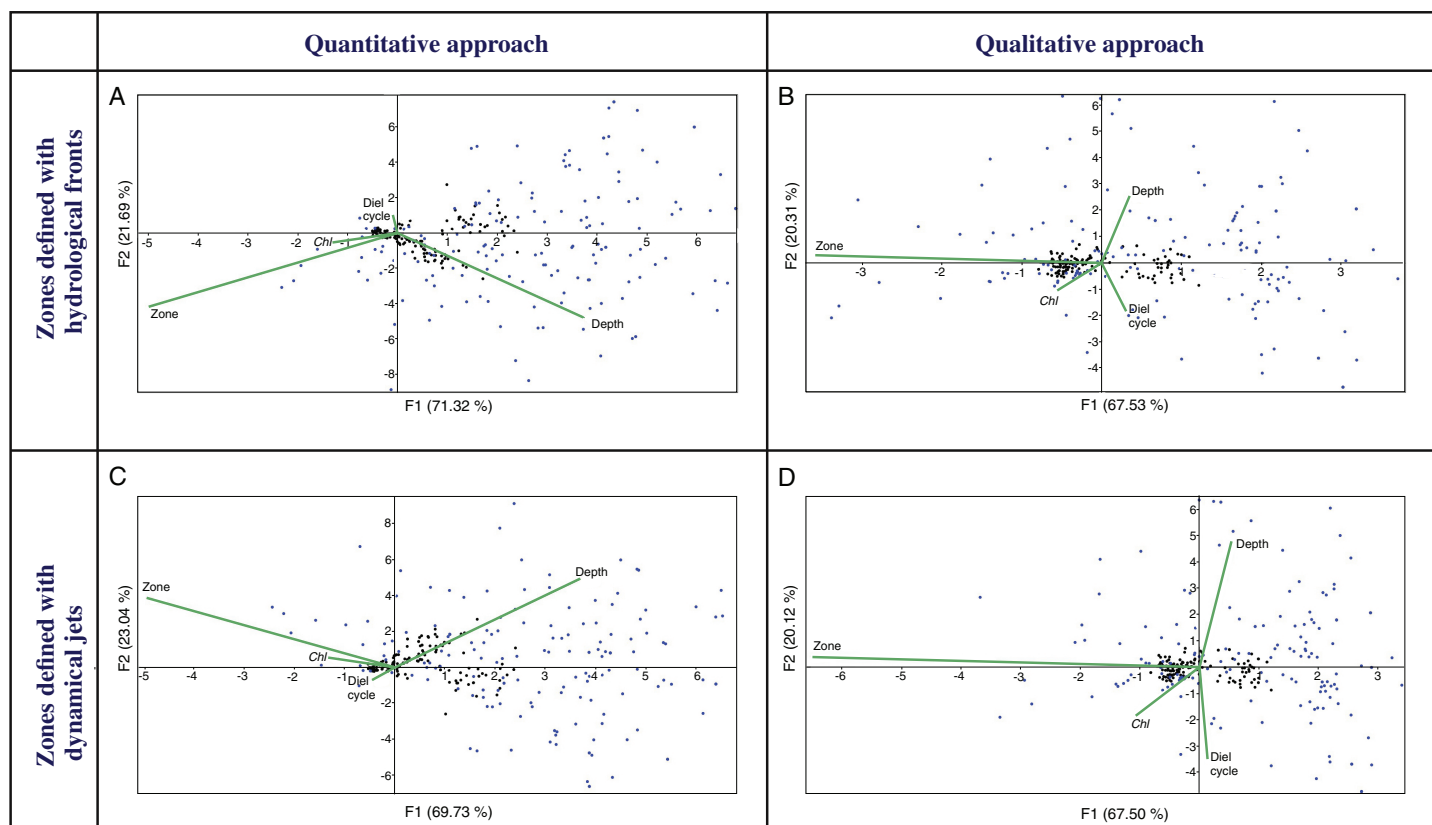
Full-size 🖼 DOI: 10.7717/peerj.11411/fig-3

Figure 4 CCAs with stations bounded by four hydrological fronts and eight dynamic jets, under quantitative data based on proportion of taxa (A and C), stations bounded by four hydrological fronts and qualitative data based on presence/absence of taxa (B and D), stations bound. Two first axes (F1 and F2) with respective variance are represented. Environmental variables: hydrological zone (Zone), depth layer (Depth), surface chlorophyll averaged over the month of the survey (December) and over a 1° (latitude) × 5° (longitude) rectangle with the sampling site in the centre (*Chl*), and diel cycle conditions (Diel cycle). Black circles indicate position of samples, and blue circles indicate position of taxa.

Full-size 🖼 DOI: 10.7717/peerj.11411/fig-4

When we divided plankton assemblages into nine groups bounded by jets and used the qualitative approach, the boundary effect was weaker and only a few combinations passed tests (ANOSIM tests in Table 4 and MDS scaling in Appendix 5): the STF in all layers, and the PF, the SACCF-N, and the SACCF-S in some layers. The SAF-N, the SAF-M, the SAF-S, and the SB jets did not provide statistically significant boundaries. Quantitative results (Appendix 6) indicated a significant difference in the boundary effect only twice: the STF (the deep layer) and the SACCF-S (upper layer).

Cluster analyses confirmed the results of the discontinuity approach and ANOSIM tests. The qualitative approach retrieved a strong separating effect of all hydrological fronts

Table 2 Results of the pairwise tests (two-way ANOSIM) used to identify significant differences between plankton assemblages sampled in different depth layers (Depth), hydrological zones (Zone) divided by four fronts or eight jets, during different diel cycles (Diel), and in different productive zones (*Chl*). Combinations Zone-*Chl* are not included due to insufficient group level combinations. Significant *p*-values are in bold.

Pairwise test	Factors	Bray-Curtis quantitative	Bray-Curtis qualitative
Depth-Zone (four fronts)	Depth, p	**0.0001**	**0.0001**
	Zone, p	**0.0001**	**0.0001**
Depth-Zone (eight jets)	Depth, p	**0.0001**	**0.0001**
	Zone, p	**0.0001**	**0.0001**
Diel-Zone (four fronts)	Diel, p	0.8306	0.5855
	Zone, p	**0.0001**	**0.0001**
Diel-Zone (eight jets)	Diel, p	0.8722	0.2573
	Zone, p	**0.0050**	**0.0001**
Diel-Depth (four fronts)	Diel, p	0.6509	0.6359
	Depth, p	**0.0001**	**0.0072**
Diel-Depth (eight jets)	Diel, p	0.8013	0.4202
	Depth, p	**0.0001**	**0.0015**
Chl-Diel (four fronts)	Chl, p	**0.0041**	**0.0002**
	Diel, p	0.148	0.6889
Chl-Diel (eight jets)	Chl, p	**0.0040**	**0.0002**
	Diel, p	0.1249	0.5493
Chl-Depth (four fronts)	Chl, p	**0.0031**	**0.0001**
	Depth, p	**0.0001**	**0.0002**
Chl-Depth (eight jets)	Chl, p	**0.0031**	**0.0009**
	Depth, p	**0.0001**	**0.0002**

on QUAL-structure of assemblages, except the SB (visible in all layers and in the whole 0–300 m layer–Figs. 6–7, Appendices 7–9). In the whole 0–300 m layer, four statistically significant clusters fitted four distinct assemblages between the fronts, while assemblages in the individual layers between the fronts were in some cases represented by one to three subclusters. The deepest node in cladograms always corresponded to the STF, suggesting the greatest separating effect by this front. It is notable that two 0–300 m samples (black dots) from the plankton gap in the warm core eddy were not grouped with other samples.

The quantitative approach showed that the effect of all hydrological fronts on QNT-structure of assemblages is present but obscure (Fig. 8, Appendices 10–11). For example, the left robust cluster at similarity level ~38 (Fig. 8) includes mainly South stations (south of the PF) interrupted by three North-Central stations (between the STF and the SAF) and a single Central station (between the SAF and the PF–Fig. 8). The right robust clade at similarity level ~38 (Fig. 8) encompasses mostly North stations (north of the STF) along with two Central stations.
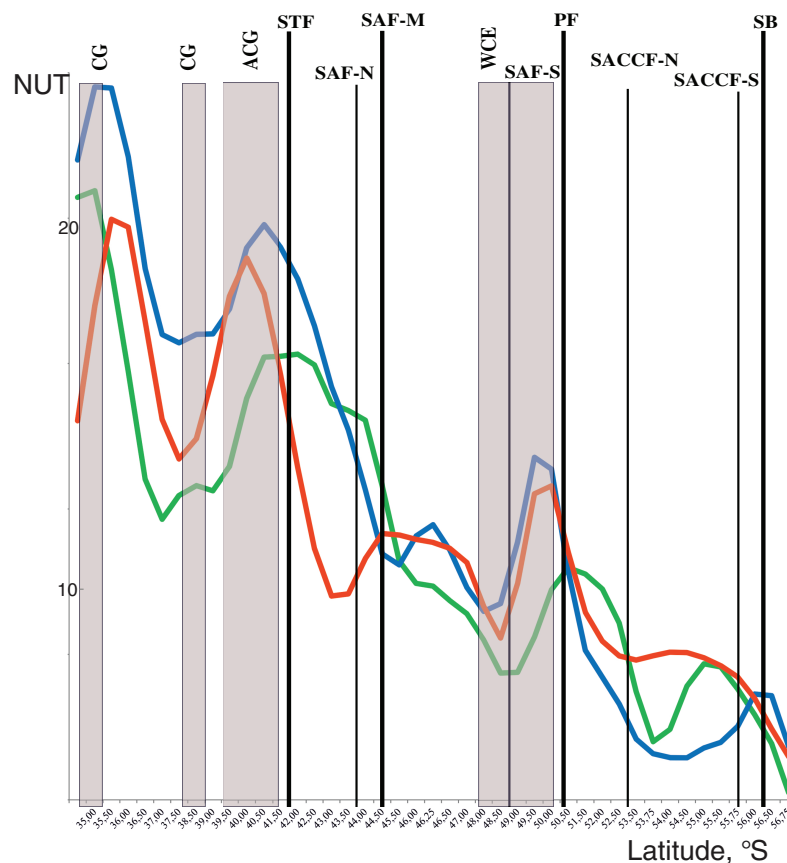
Figure 5 Discontinuity of plankton assemblages along transect: number of unique taxa respective neighboring stations (NUT). Gaussian smoother for nine points used for upper layer (green line), intermediate layer (blue line), and deep layer (red line). Hydrological coding (vertical black lines): Subtropical Front (STF); Subantarctic Front (SAF), three branches (northern SAF-N, middle SAF-M and southern SAF-S); Polar Front (PF), merged branches; Southern ACC Front (SACCF), two branches (northern SACCF-N and southern SACCF-S); Southern Boundary (SB), cyclonic gyre (CG), anticyclonic gyre (ACG) and warm core eddy (WCE). Hydrological fronts are indicated by thicker lines.

Full-size 🖼 DOI: 10.7717/peerj.11411/fig-5

Tables 5 and 6 show taxa, which contributed in differences between mesoplankton communities within the 0–300 m layer bounded by hydrological fronts. Differences in QUAL-structure are supported mainly by copepods (99 taxa) and, to a lesser extent, by amphipods (7 taxa). Differences in QNT-structure of assemblages are mainly explained by 11 copepod taxa (a total of ~70 %, with a leading role of *Oithona similis*), and unidentified Euphausiacea, Appendicularia, Foraminifera, and Radiolaria (2–4% each group).

DISCUSSION

Composition of zooplankton assemblages and distribution of dominant taxa

The cyclopoid *O. similis* was the most abundant species composing nearly half of the total mesoplankton abundance, which is likely explained by the time period surveyed (late spring-early summer), which is when the abundance of this species is maximal (*Hosie*

Table 3 Results of the ANOSIM tests to identify differences between plankton assemblages bounded by hydrological fronts (Bray-Curtis qualitative index used). Tested layers: upper mixed (Layer 1), intermediate (Layer 2), deep (Layer 3), and the whole 0-300 m layer (Layer 0). Zones: north of STF (1), between STF and SAF-M (2), between SAF-M and PF (3), between PF and SB (4), and south of SB (5). Statistically significant boundaries between neighboring zones are in bold.

Layer 1

	2	3	4	5
1	**0.0002**	**0.0001**	**0.0001**	**0.0015**
2		**0.0006**	**0.0004**	**0.009**
3			**0.0002**	**0.0035**
4				0.0674

Layer 2

	2	3	4	5
1	**0.0002**	**0.0001**	**0.0001**	**0.0022**
2		**0.0363**	**0.0001**	**0.009**
3			**0.0001**	0.2921
4				**0.0135**

Layer 3

	2	3	4	5
1	**0.0002**	**0.0001**	**0.0001**	**0.0017**
2		0.2198	**0.0001**	**0.0082**
3			**0.0002**	0.2998
4				0.0691

Layer 0

	2	3	4	5
1	**0.0001**	**0.0001**	**0.0001**	**0.0019**
2		**0.0018**	**0.0001**	**0.0068**
3			**0.0001**	**0.0441**
4				0.1205

et al., 2014). A high abundance of *O. similis* was previously recorded during the same time period (*Stupnikova et al., 2018*; *Vedenin et al., 2019*; *Žmijevska, 1987*), whereas in other seasons the contribution of this species was significantly lower (e.g., *Atkinson & Peck, 1988*; *Pakhomov et al., 2000*; *Pakhomov & McQuaid, 1996*; *Takahashi et al., 2010*). Other abundant taxa such as unidentified young calanoid copepodites, euphausiid nauplii, *Ctenocalanus citer*, and Foraminifera, were dominant in our samples and are known to be common in the Southern Ocean (*Voronina, 1984*; *Vervoort, 1965*; *Bradford, 1969*, *1971*). Overall, the abundance of dominant taxa and biodiversity were distributed relatively homogenously across the ACC region except a plankton-depleted area at ~49° S.

The list of taxa identified in our samples aligns with previous records from the Southern Ocean (*Mackintosh, 1937*; *Pakhomov et al., 2000*, *Pakhomov & Froneman, 2004a*, *2004b*;

Table 4 Results of the ANOSIM tests to identify differences between plankton assemblages bounded by jets (Bray-Curtis qualitative index used). Tested layers: upper mixed (Layer 1), intermediate (Layer 2), deep (Layer 3), and the whole 0-300 m layer (Layer 0). Zones: north of STF (1), between STF and SAF-N (2), between SAF-N and SAF-M (3), between SAF-M and SAF-S (4), between SAF-S and PF (5), between PF and SACCF-N (6), between SACCF-N and SACCF-S (7), between SACCF-S and SB (8), and south of SB (9). Statistically significant boundaries between neighboring zones are in bold.

Layer 1

	2	3	4	5	6	7	8	9
1	**0.0017**	**0.0093**	**0.0001**	**0.0002**	**0.0004**	**0.0001**	**0.0014**	**0.0026**
2		0.8931	**0.0009**	**0.0089**	**0.0077**	**0.0013**	**0.0185**	**0.0197**
3			0.2753	0.068	**0.0345**	**0.0124**	0.0996	0.1057
4				0.3961	**0.0089**	**0.0016**	**0.008**	**0.0055**
5					**0.0363**	**0.0024**	**0.0335**	**0.0196**
6						0.1725	0.1877	0.0505
7							**0.0363**	**0.012**
8								0.3884

Layer 2

	2	3	4	5	6	7	8	9
1	**0.0006**	**0.0026**	**0.0001**	**0.0001**	**0.0002**	**0.0001**	**0.0014**	**0.002**
2		0.8194	**0.0328**	**0.0183**	**0.0074**	**0.0014**	**0.0348**	**0.0163**
3			0.4522	0.1986	**0.0194**	**0.0117**	0.1006	0.1017
4				0.3213	0.212	0.0557	0.7609	0.1329
5					**0.0388**	**0.0025**	0.2827	0.1796
6						**0.0077**	**0.0182**	**0.0158**
7							0.0844	**0.0129**
8								0.499

Layer 3

	2	3	4	5	6	7	8	9
1	**0.0004**	**0.0026**	**0.0001**	**0.0003**	**0.0001**	**0.0001**	**0.0017**	**0.0015**
2		0.3006	0.1063	**0.017**	**0.0085**	**0.0021**	**0.0172**	**0.0164**
3			0.773	0.5125	**0.0186**	**0.0105**	0.1022	0.1034
4				0.1771	0.2611	**0.0176**	0.2493	0.1615
5					0.1573	**0.0042**	0.2679	0.3388
6						0.1515	**0.0183**	**0.0178**
7							**0.047**	**0.0252**
8								0.3062

Layer 0

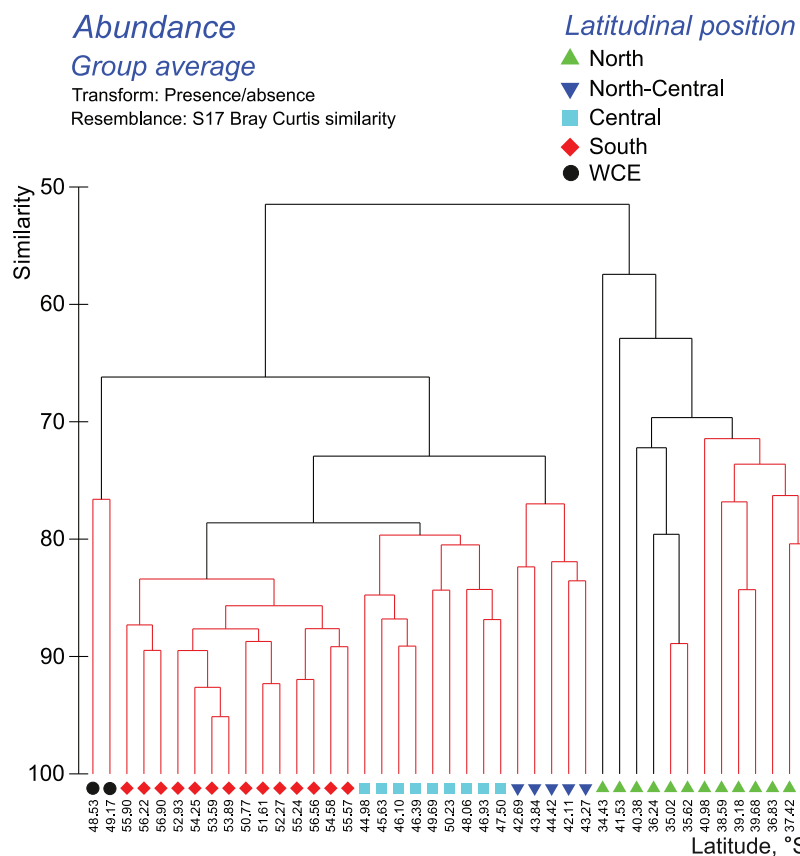|	2	3	4	5	6	7	8	9
1	**0.0003**	**0.0017**	**0.0001**	**0.0002**	**0.0001**	**0.0001**	**0.0025**	**0.0016**
2		0.4412	**0.0019**	**0.0088**	**0.0069**	**0.0018**	**0.035**	**0.0173**
3			0.0743	0.1217	**0.0196**	**0.0102**	0.099	**0.1001**
4				0.0511	**0.003**	**0.0007**	**0.013**	**0.0128**
5					0.0853	**0.0023**	0.1218	0.1457
6						**0.0487**	**0.019**	**0.0183**
7							**0.0228**	**0.0119**
8								0.3976

Figure 6 Results of the cluster analysis (Bray–Curtis qualitative index) of samples collected within the upper 300-m layers. Colored lines and nodes indicate robust (black, $p < 0.05$) and statistically insignificant (red, $p > 0.05$) clusters. Colored figures on bottom indicate robust clusters. Black dots indicate samples not grouped with other clusters.　　　　Full-size 🖼 DOI: 10.7717/peerj.11411/fig-6

Froneman, 2000; *Stupnikova & Vereshchaka, 2013*; *Voronina, 1984*). The list is expected to include most mesoplankton taxa occurring in the Southern Ocean because seasonal upward migrations had generally occurred by the time of our survey (austral summer) (*Hardy & Gunther, 1935*; *Mackintosh, 1934*; *Voronina, 1984*; *Rudjakov & Voronina, 1973*) and mesoplankton typically concentrate in the sampled 0–300 m layer to feed and to reproduce (*Gliwicz, 1986*; *Żmijevska, 1987*; *Lampert, 1989*; *Park & Ferrari, 2009*).

Surprisingly, composition of zooplankton assemblages and distribution of dominant taxa remained relatively stable during at least 17 years. In fact, our results generally align with the data from the same transect in the late austral summer of 1992/1993 (*Pakhomov et al., 2000*). Variations in abundance, distribution, taxa richness, and bounding effects of the basic hydrological fronts are similar, which suggests a long-term stability of the basic mesoplankton characteristics along this transect. The surveys in 1993 and 2009 mainly differed in the sampling method: Bongo net and a single 0–300 m sample per station in 1993 and Judey net and three discrete layers per station in 2009. In addition, seasons were slightly different (December in 2009 vs. January–February in 1993). In 2009, the total abundance of mesoplankton in discrete layers along the transect ranged from 0.2 ind. m^{-3} to 13,743.6 ind. m^{-3} (five orders of magnitude), maximal and
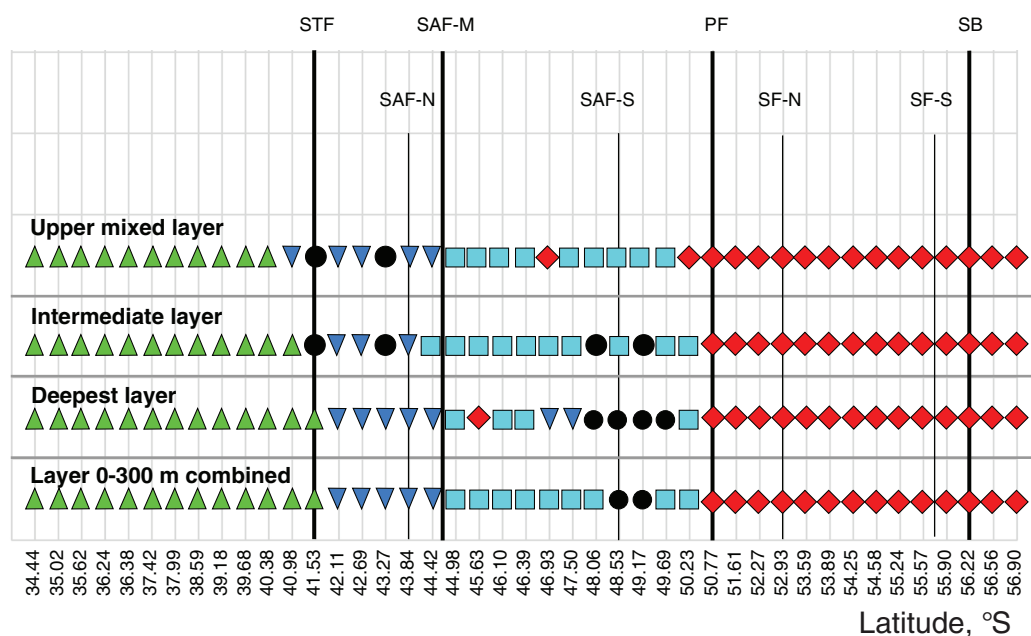
Figure 7 **Distribution of the retrieved clusters (Bray-Curtis qualitative index, Fig. 6) along transect.** Hydrological jet coding (vertical black lines): Subtropical Front (STF); Subantarctic Front (SAF), three branches (northern SAF-N, middle SAF-M and southern SAF-S); Polar Front (PF), merged branches; Southern ACC Front (SACCF), two branches (northern SACCF-N and southern SACCF-S); and Southern Boundary (SB). Hydrological fronts are shown by thicker lines. Colors indicate groups diverging at certain similarity levels. Black dots indicate samples not grouped with other clusters.

Full-size 🖾 DOI: 10.7717/peerj.11411/fig-7

minimal values were recorded in the upper mixed and in the deepest layer, respectively. Within the combined 300-m layer, averaged abundances ranged from 16 to 1,455 ind. m^{-3} (two orders of magnitude). Consequently, total 0–300 m samples provide little information about actual variations of mesoplankton abundances within this layer.

In 1993, values for the same 0–300 m layer were one order of magnitude lower than in 2009 but variations were same (two orders of magnitude), from 2.1 to 211.5 ind. m^{-3}. Judey nets are known to provide an order of magnitude higher mesoplankton abundance than Bongo nets (*Voronina, 1984*; *Fransz & Gonzalez, 1997*) and comparison of both surveys confirmed this finding. Maximal difference between surveys of 2009 (Judey net with mesh 0.18 mm) and 1993 (Bongo net with mesh 0.30 mm) was observed in the smallest fraction (*Oithona*, *Oncaea*, etc.), which likely passed through coarser Bongo mesh. Interestingly, the range of abundances, i.e., two orders of magnitude, remains constant regardless the net type and thus may be characteristic for mesoplankton of the Southern Ocean.

Both surveys showed similar local enrichments of mesoplankton abundance near the PF and the SAF, but differed in other patterns. A local peak north of the STF associated with the Agulhas Retroflection Current and found in 1993 was missing in 2009. Instead, local enrichments were recorded south and north of the STF, and were merely associated with mesoscale variability of the STF (Figs. 2A, 3A).
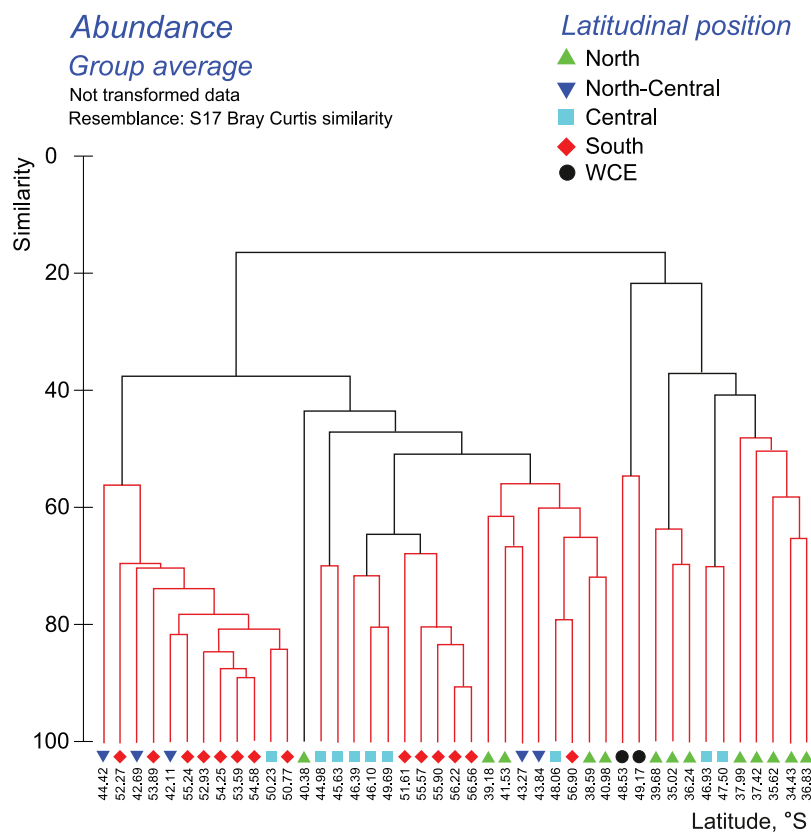
Figure 8 Results of the cluster analysis (Bray–Curtis quantitative index) of samples collected within the upper 300-m layers. Colored lines and nodes indicate robust (black, $p < 0.05$) and statistically insignificant (red, $p > 0.05$) clusters. Colored figures as in Fig. 6.

Full-size ⊡ DOI: 10.7717/peerj.11411/fig-8

The next local peak near the northernmost position of the zero isotherm was narrow in 1993 and expanded over a wider latitudinal range (52° S–55.5° S) in 2009 (Fig. 3A here). This difference was likely induced by a greater advection of cold waters in 2009 (earlier survey season) relative to 1993.

Surprisingly, the survey in 2009 yielded nearly the same number of taxa as in 1993 (162 taxa in 1993 vs. 163 taxa in 2009). Thus, even significant difference in mesh size and net opening did not affect qualitative composition of mesoplankton. Conversely, different nets resulted in greatly different QNT-structure and the lists of dominant taxa. Among 15 most abundant taxa recorded in 1993 and 2009 (Table 2 here), only five taxa are common: *Oithona* sp., *Oncaea* sp., *Ctenocalanus* sp., *Clausocalanus* sp., and *Pleuromamma* sp. Like in 1993, taxa richness for the majority of stations varied between 15 and 25 taxa per station (Fig. 2E here). *Pakhomov et al. (2000)* indicated "slightly elevated number of taxa associated with … APF, SAF, STC and Agulhas Retroflection Current" but their Fig. 4A does not support this conclusion. Like Fig. 4A of *Pakhomov et al. (2000)*, our Fig. 2E does not show any significant increase of taxa richness near any front or jet. The only visible trend is associated with an increase of taxa richness north of the STF (Fig. 2E) owing to a diversity of small subtropical copepods in mesoscale eddies of the

Table 5 List of taxa contributing to differences between mesoplankton assemblages bounded by four hydrological fronts, qualitative approach based on presence/absence of taxa (retrieved in Figs. 6–7). 1/0–present/absent within assemblages.

Species	Presence/Absence			
	North	North-Central	Central	South
Copepoda				
Clausocalanus brevipes	1	1	1	0
Pareucalanus langae	1	1	1	0
Calocalanus sp.	1	1	0	0
Calocalanus contractus	1	1	0	0
Calocalanus pavo	1	1	0	0
Candacia catula	1	1	0	0
Corycaeus furcifer	1	1	0	0
Lucicutia flavicornis	1	1	0	0
Neocalanus gracilis	1	1	0	0
Phaenna spinifera	1	1	0	0
Pleuromamma gracilis	1	1	0	0
Pleuromamma quadrungulata	1	1	0	0
Scolecithrix bradyi	1	1	0	0
Aetideus giesbrechti	1	0	1	1
Calanoides acutus	1	0	1	1
Haloptilus longicornis	1	0	1	1
Aetideus australis	1	0	1	0
Oithona nana	1	0	1	0
Lubbockia squillimana	1	0	0	1
Scolecithricella glacialis	1	0	0	1
Acartia longiremis	1	0	0	0
Aegistus dubius	1	0	0	0
Aetideopsis carinata	1	0	0	0
Aetideus acutus	1	0	0	0
Calocalanus styliremis	1	0	0	0
Calocalanus tenuis	1	0	0	0
Candacia sp.	1	0	0	0
Candacia varicans	1	0	0	0
Centropages bradyi	1	0	0	0
Centropages gracilis	1	0	0	0
Centropages violaceus	1	0	0	0
Chiridius gracilis	1	0	0	0
Chirundina streetsii	1	0	0	0
Clausocalanus arcuicornis	1	0	0	0
Clausocalanus pergens	1	0	0	0
Clausocalanus sp.	1	0	0	0
Corycaeus giesbrechti	1	0	0	0
Corycaeus limbatus	1	0	0	0

(Continued)

Table 5 (continued)				
Species	**Presence/Absence**			
	North	**North-Central**	**Central**	**South**
Corycaeus speciosus	1	0	0	0
Ctenocalanus vanus	1	0	0	0
Eucalanus elongatus elongatus	1	0	0	0
Eucalanus hyalinus	1	0	0	0
Euchaeta acuta	1	0	0	0
Euchirella intermedia	1	0	0	0
Euchirella sp.	1	0	0	0
Farranula rostrata	1	0	0	0
Gaetanus miles	1	0	0	0
Gaetanus minor	1	0	0	0
Haloptilus spiniceps	1	0	0	0
Heterorhabdus robustus	1	0	0	0
Heterostylites major	1	0	0	0
Lophothrix latipes	1	0	0	0
Lucicutia clausi	1	0	0	0
Lucicutia curta	1	0	0	0
Lucicutia ovalis	1	0	0	0
Macrosetella gracilis	1	0	0	0
Mesocalanus tenuicornis	1	0	0	0
Nannocalanus minor	1	0	0	0
Nullosetigera helgae	1	0	0	0
Oculosetella gracilis	1	0	0	0
Oncaea sp.	1	0	0	0
Onychocorycaeus giesbrechti	1	0	0	0
Paracalanus parvus parvus	1	0	0	0
Paraheterorhabdus robustus	1	0	0	0
Pareuchaeta bisinuata	1	0	0	0
Pareuchaeta sp.	1	0	0	0
Pareuchaeta tonsa	1	0	0	0
Rhincalanus nasutus	1	0	0	0
Sapphirina sp.	1	0	0	0
Sapphirina angusta	1	0	0	0
Scaphocalanus sp.	1	0	0	0
Scolecithrix danae	1	0	0	0
Scottocalanus persecans	1	0	0	0
Scottocalanus securifrons	1	0	0	0
Spinocalanus brevicaudatus	1	0	0	0
Subeucalanus longiceps	1	0	0	0
Subeucalanus monachus	1	0	0	0
Undinula vulgaris	1	0	0	0

Table 5 (continued)

Species	Presence/Absence			
	North	North-Central	Central	South
Valdiviella minor	1	0	0	0
Candacia maxima	0	1	1	1
Clausocalanus laticeps	0	1	1	1
Clytemnestra rostrata	0	1	1	1
Heterorhabdus papilliger	0	1	1	1
Pareuchaeta biloba	0	1	1	0
Candacia cheirura	0	1	0	0
Pareuchaeta gracilis	0	1	0	0
Pleuromamma robusta	0	1	0	0
Metridia gerlachei	0	0	1	1
Euchirella truncata	0	0	1	0
Gaetanus robustus	0	0	1	0
Lucicutia lucida	0	0	1	0
Mormonilla minor	0	0	1	0
Pareuchaeta sarsi	0	0	1	0
Undeuchaeta plumosa	0	0	1	0
Aetideopsis rostrata	0	0	0	1
Clausocalanus furcatus	0	0	0	1
Haloptilus ocellatus	0	0	0	1
Heterorhabdus compactus	0	0	0	1
Lubbockia aculeata	0	0	0	1
Amphipoda				
Phronima sp.	1	1	1	0
Cyphocaris sp.	1	1	0	0
Eupronoe sp.	1	0	0	0
Rhabdosoma sp.	1	0	0	0
Streetsia sp.	1	0	0	0
Vibilia sp.	1	0	0	0
Themisto sp.	0	0	0	1
Bivalvia larvae	1	0	1	0
Bryozoa larvae	1	0	0	0
Cephalopoda larvae	1	0	0	0
Decapoda larvae	1	1	1	0
Echinodermata larvae	1	0	0	1
Gastropoda larvae	1	0	0	1
Mysidacea *Echinomysis*	0	0	0	1
Polychaeta larvae	1	1	0	0
Salpidae	1	0	1	0

Note:
Taxa sorted by major taxonomic groups then by presence in North assemblage, etc.

Table 6 List of taxa contributing to differences between mesoplankton assemblages bounded by four hydrological fronts, quantitative approach based on proportion of taxa (retrieved in Figs. 6–7).

Species	Average abundance				Average dissimilarity	Dissimilarity/ SD	Contribution (%)
	North	North-Central	Central	South			
Copepoda							
Oithona similis	148.67	646.95	303.15	915.04	26.71	1.66	39.87
Copepoda copepodites	43.81	220.11	89.41	200.1	7.21	1.51	10.86
Ctenocalanus citer	0.05	48.04	50.08	94.35	3.35	1.22	4.98
Microcalanus pusillus	25.12	69.89	5.31	37.07	2.85	0.90	4.28
Triconia antarctica ♂	0.27	2.52	7.11	46.85	1.24	1.28	1.91
Clausocalanus brevipes	11.34	32.89	11.62	0	1.09	1.20	1.64
Clausocalanus pergens	27.47	0	0	0	1.04	1.00	1.40
Paracalanus parvus parvus	21.77	0	0	0	0.87	0.69	1.17
Pleuromamma gracilis	21.79	0.97	0	0	0.83	0.83	1.12
Oncaea sp.	24.44	0	0	0	0.80	0.75	1.08
Calanus propinquus	0.71	16.94	0.03	1.64	0.62	0.74	0.96
Euphausiacea nauplii	2.62	82.24	36.99	88.67	3.31	1.10	4.99
Appendicularia	2.34	121.91	21.64	9.58	2.82	0.79	4.36
Foraminifera	10.2	38.57	27.87	107.36	2.81	1.30	4.24
Radiolaria	0.29	65.92	13.1	23.04	1.65	0.77	2.56

Note:
  SIMPER analysis, species are arranged according major groups and further to their mean contribution. The list is cut at a 1% of contribution.

Agulhas Current (compare Figs. 2A, 2B and Fig. 2E). Shannon (*H*) and Dominance (*D*) indices in 2009 (Figs. 2C, 2D) also do not show any visible trends along the transect (but show increase in biodiversity with depth). Regrettably, these indices were not presented in *Pakhomov et al. (2000)*.

In both surveys, the basic separation of stations according to taxonomic composition of zooplankton in the whole layer 0–300 m coincided with the position of the STF, the SAF, and the PF. Despite the use of different sampling methods in 1993 and 2009, this basic grouping of plankton assemblages was not biased. As in 2009, secondary clusters were observed in 1993, but they are difficult to interpret because some stations were excluded from Fig. 6 of *Pakhomov et al. (2000)*.

Overall, comparison of both surveys shows the existence of similar and stable plankton assemblages along the ST02 transect during a period 1992–2009. Similar spatial variations in abundance, distribution, taxa richness, and bounding effects of the basic hydrological fronts were found in both surveys regardless the sampling gear. Observed differences may be referred to sampling gear and temporal hydrological variability along the transect. In spite of observed spatio-temporal variability of mesoplankton, three principal hydrological fronts (the STF, the SAF, and the PF) represent clear biogeographic boundaries, which are detected on various size groups sampled by different gears.

Comparative impact of major environmental factors on mesoplankton abundance and biodiversity

Although zooplankton assemblages in the Southern Ocean are influenced by various environmental factors, including temperature, ocean acidification, depth, thickness of sea ice, etc. (e.g., reviewed by *Constable et al., 2014*), the most notable factors are believed to be hydrological fronts and depth (*Pakhomov, Perissinotto & McQuaid, 1994*, *Pakhomov et al., 2000*; *Pakhomov & Froneman, 2004a*, *2004b*; *Froneman, 2000*; *Vedenin et al., 2019*, *2020*; *Pakhomov & McQuaid, 1996*; *Pinkerton et al., 2002*; *Smetacek et al., 2002*). Sea ice and climate indices may also be notable drivers but their impact have been so far recorded close to the Antarctic continent (*Steinberg et al., 2015*; *Thibodeau et al., 2019*).

Our analyses of abundance, biodiversity and QUAL-structure of mesoplankton in the Southern Ocean transect SR02 confirm the importance of hydrological factors and sampled depth and provide a deeper insight into the hierarchy of environmental factors affecting these characteristics.

Our results indicate that depth greatly influences abundance, biodiversity, and QNT-structure of mesoplankton. Dominant taxa aggregate mostly in the upper mixed layer (Figs. 3B–3F); as a result, total plankton abundance (Fig. 3A) is also highest near the surface. This distribution mirrors vertical profiles of primary production, which is highest in the upper layer and decreases with the depth (*Demidov, Mosharov & Gagarin, 2012*). The vertical distribution of biodiversity indices has an opposite trend and increases with depth (Figs. 2C–2E). The upper mixed layer is dominated by few abundant taxa (Figs. 3B–3F), while the deepest layer is inhabited by a greater number of taxa more equally represented, which results in an increase of Shannon (H) and in a decrease of Dominance (D) indices with depth (Figs. 2C, 2D). Being a driver of abundance and biodiversity, depth greatly influences a QNT-structure of planktonic assemblages, but only slightly affects QUAL-structure depending on presence/absence of taxa (in the 0–300 m layer most taxa are recorded at all depths).

Hydrological zone strongly affects QUAL-structure and QNT-structure of mesoplankton assemblages. When we analyze QUAL-structure in CCAs (Figs. 4B, 4D) and ANOSIM tests (Table 2), hydrological zone becomes a dominant factor, regardless of the zone separation method (front or jets). A specific combination of environmental factors, such as temperature, salinity, etc., associated with each individual hydrological zone (water mass), affects QUAL-structure more than any other factor (the effect of depth is negligible in this case because most taxa occur throughout all sampled depth, although in different numbers). The effect of hydrological zone on QNT-structure of assemblages (linked to taxa proportions in samples) is less remarkable and comparable with the effect of depth (Figs. 4A, 4C).

Hydrological zone does not appear to notably affect distribution of mesoplankton abundance and biodiversity within the ACC area. The increase of abundance at 40° S (total abundance, abundance of *O. similis* and calanoid copepodites–Figs. 2A–2C) is likely linked to an anticyclonic eddy (part of the Agulhas meander), which incorporated Subantarctic waters of the ACC origin (details in *Tarakanov & Gritsenko, 2014*). A striking

decrease in mesoplankton abundance around 49° S, especially prominent in the intermediate and deep layers (Figs. 3A–3E), is likely associated with a local increase of temperature and decrease of salinity in the same layers (Figs. 2A, 2B) and with the presence of a mesoscale warm core eddy. This eddy was recorded only in the intermediate and deepest layers, not in the upper mixed layer and not on a satellite image (we show the conditional position of this eddy in Fig. 1). The subsurface eddy was not considered by *Tarakanov & Gritsenko (2014)*, its origin and genesis are unclear. Anyway, local effect of this eddy is visible in distribution of all mesoplankton characteristics and also mirrored in two stations, which greatly differed in QUAL- and QNT-structure from all recorded assemblages (black dots in Fig. 6). Interestingly, *Chl* measured in situ (*Demidov, Mosharov & Gagarin, 2012*) was also minimal within this zone. We only may suppose that the decrease of mesoplankton abundance may be related to a long-living eddy and to a consequent advection of deep plankton-depleted waters. Like abundances, biodiversity indices are more or less similar across various hydrological zones, except the northern stations within the core of the Agulhas Current (Indian Ocean species added) and the plankton-depleted area around 49° S discussed above. Thus, we did not find any significant effect of continuous hydrological fronts on biodiversity indices, even near the PF.

In this paper, we first tested productivity (*Chl*) as a possible driver of mesoplankton composition in the Southern Ocean. We understand that satellite *Chl* estimations are not ideal due to the lack of inclusion of sub-surface maxima and imperfection of algorithm calculations, which may lead to biased values (*Garcia, Garcia & McClain, 2005*; *Zeng, Xu & Fischer, 2016*; *Brewin et al., 2017*). However, potential impacts of productivity on integral characteristics of zooplankton could be identified by using *Chl* as a proxy of phytoplankton productivity and biomass (*Vereshchaka et al., 2016*, *2017*; *Vereshchaka, Lunina & Sutton, 2019*). In our dataset, *Chl* is the third factor (after hydrological zone and depth) influencing the QNT-structure (Figs. 4A, 4C). Mesoplankton ascend to the surface for feeding and reproduction (*Gliwicz, 1986*; *Żmijevska, 1987*; *Lampert, 1989*; *Park & Ferrari, 2009*). As the amount of food affects abundance rather than presence/absence of taxa, QNT-structure of mesoplankton is much more dependent on *Chl* than QUAL-structure. In fact, along the OX axis explaining the main part of variance, the *Chl* vector is 0.28 % of the Zone-vector length under the quantitative approach (Fig. 4C) and only 0.16% of the Zone-vector length under the qualitative approach.

The fourth analyzed factor, diel cycle, is nearly negligible in CCAs (Figs. 4A–4D) and not statistically significant in the ANOSIM tests (Table 2), meaning day and night samples do not differ and diel migrations are not definite in our dataset. These results are in accordance with data of *Pakhomov et al., 2000*, which did not find significant differences in zooplankton densities between samples collected during the daytime and nighttime ($P > 0.05$). Studies on *Calanus acutus* (*Hardy & Gunther, 1935*) and *C. propinquus* (*Mackintosh, 1934*; *Voronina, 1984*; *Rudjakov & Voronina, 1973*) did not record diel migrations in the summer period as well. However our data do not suggest a complete absence of diel migrations for mesoplankton. More robust datasets (*Vedenin et al., 2020*) or other methods with greater vertical resolution (*Vinogradov et al., 1996*; *Conroy et al., 2020*) confirm diel migrations of low amplitude during the polar summer.

Interestingly, even our dataset provides some evidence for diel migrations. In all CCAs plots (Figs. 4A–4D), diel cycle is opposed to depth (i.e., many taxa tend to occur at a lesser depth at night). While this effect is present in our study, it is not statistically significant, which suggests that diel cycle is the weakest among all of the analyzed factors.

Comparative impact of hydrological fronts and jets on mesoplankton abundance and biodiversity

The hydrological fronts have varying effects on the mesoplankton. The STF divides subtropical and subpolar fauna and thus has the strongest impact. The vicinities of the STF were previously recognized as a transitional zone between the Subantarctic and the Subtropical Zones (*McGinnis, 1977*; *Lomakina, 1964*) with eddies and meanders causing local discontinuities in species distribution, which are also visible in our dataset (Fig. 5, north of the STF). The dominating impact of the STF is confirmed by a statistically significant difference between assemblages north and south of this front (Tables 3–4, Appendices 3, 5) and by clustering (least similarity in Figs. 6–7, Appendices 7–9).

The PF is the second strongest front: discontinuity of plankton assemblages is distinct (NUT–Fig. 5) and the division of neighboring assemblages is statistically robust (Table 3, Appendix 3) at all depths. However, assemblages on both sides of the PF are more similar than those on both sides of the STF (Figs. 6–7, Appendices 7–9).

The effect of the SAF is weaker than that of the STF and the PF, which may explain a current uncertainty in the literature. Indeed, the impact of the STF and the PF on plankton distribution in the Southern Ocean has been recognized for a long time (*Foxton, 1956*; *Hopkins, 1971*; *Pakhomov & McQuaid, 1996*; *Dolzhenkov, 1982*; *Deacon, 1982*; *Grachev, 1991*), whereas the role of the SAF was less certain (*Pakhomov & McQuaid, 1996*; *Pakhomov et al., 2000*). A possible explanation is that the effect of the SAF may differ depending on geographic area and/or season. In the Drake Passage, the SAF and the PF may have a subequal effect (*Hosie et al., 2014*; *Vedenin et al., 2019*), whereas in our survey the SAF does not affect distribution in the deep layer (the PF influences all sampled depths: Appendix 3, Table 3) and does not provide significant faunal discontinuity (Fig. 5).

The SB is the weakest hydrological front affecting mesoplankton only in the intermediate layer (Fig. 5, Table 3). This particular influence may be explained by an advection from the cold waters of the Weddell Sea, which exhibited negative temperature values in the intermediate layer in the time period of this survey (Fig. 2A).

Overall, we observed the following hierarchy of hydrological fronts: the STF, the PF, the SAF, and the SB. The effect of the first three fronts on plankton assemblages is strong and decreases with the depth (Table 3).

The effect of the dynamic jets, which are not associated with hydrological fronts, is less regular and weaker than that of hydrological fronts. For example, two jets of the SACCF divided plankton assemblages in the intermediate layer (SACCF-N) or in the upper and deep layers (SACCF-S) (Table 4, Appendix 5). A possible explanation of this result may be related to an intrusion of cold waters from the south: the isotherm of +1 °C located in the SACCF-S in the upper mixed layer moved north and crossed SACCF-N in the intermediate layer and then moved back south to cross the SACCF-S in the deep
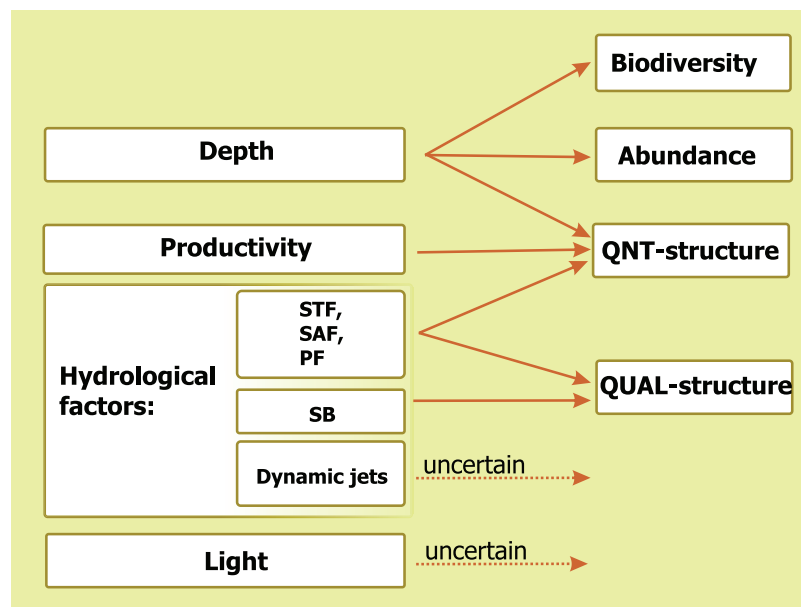
Figure 9 Concluding scheme showing the relative impact of major environmental factors and individual hydrological structures on general characteristics of plankton assemblages (white). Hydrological front coding: Subtropical Front (STF), Subantarctic Front (SAF), Polar Front (PF), and Southern Boundary (SB). Full-size ◨ DOI: 10.7717/peerj.11411/fig-9

layer (Fig. 2A). It is important to note that local eddies and meanders of various origin and evolution (*Tarakanov & Gritsenko, 2014*) may strongly affect biodiversity (Figs. 2C–2E), abundance (Fig. 3A–3F) and QUAL-structure of mesoplankton (Fig. 5). These hydrological structures may be either enriched (cyclonic gyre of the Agulhas Current north of 36° S) or depleted in mesoplankton (a warm core eddy around 49° S).

Overall, analyses of discontinuities (Fig. 5), ANOSIM tests (Tables 3, 4, Appendices 3, 5) and cluster analyses (Figs. 6–7, Appendices 7–9), all provided evidence for a strong effect of hydrological fronts and uncertain effect of dynamic jets. This result suggests that mesoplankton composition is driven by hydrological parameters and further maintained through compartmentalization by hydrological fronts.

Differences in QUAL- and QNT-structure of mesoplankton assemblages bounded by hydrological fronts are mainly explained by copepods (Tables 5–6). This is not surprising, because copepods are the most diverse and most abundant group defining the face of the mesoplankton in the Southern Ocean. Among copepods, *Oithona similis* is the most important species explaining nearly 40% of variance in QNT-structure of mesoplankton in different hydrological zones.

Concluding Remarks

Combining all three vertical strata and analyzing plankton assemblages within the whole 0–300 m layer (Fig. 6 vs. Appendices 7–9) provides a more sound output, as the dataset in this case is more representative and not biased by fluctuations in vertical distribution of taxa. At the same time, integral samples provide little information about actual variations of mesoplankton abundances. In our dataset, mesoplankton abundances

vary by five orders of magnitude in discrete vertical samples and "only" two orders of magnitude in combined 0–300 m samples.

QUAL-structure (presence or absence of taxa) of mesoplankton assemblages precisely mirrors hydrological structure: all recorded assemblages are definitely bounded by hydrological fronts. QUAL-structure is only slightly variable in time and space and may be recommended for future analyses of plankton biogeography of dynamic areas, such as the Southern Ocean. The only disadvantage of this method is related to a time-consuming identification, because ideally all taxa need to be identified to a lowest possible level (in our dataset 163 taxa). Each taxon, either rare or dominant, equally contributes to the QUAL-structure; therefore inaccurate or undetailed identification may greatly bias results. Although time-consuming, qualitative-structure may be recommended for successful biogeographic analyses of the Southern Ocean. Conversely, the quantitative approach is less sensitive to a quality of rare taxa identification and therefore less time consuming (only dominant and subdominant taxa may be identified). At the same time, QNT-structure strongly depends on proportion of taxa, which, in turn, depends on various factors, both current and precedent. Among these factors are the dynamics of particular water masses, local food resources and carnivores, life cycles in particular locations, interaction between species, etc., which may mask proper biogeographic boundaries.

A comparative impact of the analyzed environmental factors is summarized in Fig. 9. Depth influences three basic mesoplankton characteristics, hydrological factors drives two of them, *Chl* strongly affects one parameter, and diel cycle does not significantly influence any of the characteristics. The STF, the PF, and the SAF drive QNT-structure and QUAL-structure of mesoplankton (in decreasing order of influence), while the SB affects only QUAL-structure.

The basic outcome of this paper is a hierarchy of environmental factors affecting mesoplankton distribution and biodiversity. Our results show that mesoplankton composition is driven by hydrological parameters and further maintained through compartmentalization by fronts. Dynamic jets not associated with hydrological fronts have no significant effect on mesoplankton biodiversity and abundance and their position may be discarded in future hydrobiological surveys. Although characterized by two-fold fluctuations in abundances, mesoplankton distribution did not significantly change during the period 1992–2009 in the core Southern Ocean. This surprising result contrasts with recent data on climate change effect on coastal plankton assemblages of the Southern Ocean and merits new supporting/rejecting data and future surveys.

ACKNOWLEDGEMENTS

ADDITIONAL INFORMATION AND DECLARATIONS

Competing Interests

The authors declare that they have no competing interests.

Author Contributions

- Alexander Vereshchaka conceived and designed the experiments, performed the experiments, analyzed the data, prepared figures and/or tables, authored or reviewed drafts of the paper, and approved the final draft.
- Eteri Musaeva performed the experiments, identified mesoplankton taxa, and approved the final draft.
- Anastasiia Lunina performed the experiments, analyzed the data, prepared figures and/or tables, authored or reviewed drafts of the paper, and approved the final draft.

Field Study Permissions

The following information was supplied relating to field study approvals (i.e., approving body and any reference numbers):

Field works and sample collection were performed in the open ocean out of the Exclusive Economic Zones and no need any special permission or approval.

Data Availability

The following information was supplied regarding data availability:

Coordinates of stations, biomass measurements, temperature & salinity data, and MDS data are available in the Supplemental File.

Supplemental Information

Supplemental information for this article can be found online at http://dx.doi.org/10.7717/peerj.11411#supplemental-information.

REFERENCES

Accornero A, Gowing M. 2003. Annual sedimentation pattern of zooplankton fecal pellets in the southern Ross Sea: what food webs and processes does the record imply? In: *Biogeochemistry of the Ross Sea*, Vol. 78. 261–278.

Atkinson A. 1998a. Life cycles strategies of Andrews, K.J.H. The distribution and life history of Calanoides acutus (Giesbrecht). *Discovery Report* **34**:l–116.

Vereshchaka et al. (2021), *PeerJ*, DOI 10.7717/peerj.11411

30/35

Atkinson A, Peck JM. 1988. A summer-winter comparison of zooplankton in the oceanic area around South Georgia. *Polar Biology* **8(6)**:63–473 DOI 10.1007/BF00264723.

Atkinson A. 1991. Life cycles of *Calanoides acutus, Calanus simillimus* and *Rhincalanus gigas* (Copepoda: Calanoida) within the Scotia Sea. *Marine Biology* **109(1)**:79–91 DOI 10.1007/BF01320234.

Atkinson A. 1998b. Life cycles strategies of epipelagic copepods in the Southern Ocean. *Journal of Marine Systems* **15(1–4)**:289–311 DOI 10.1016/S0924-7963(97)00081-X.

Bradford J. 1969. New species of *Aetideopsis* Sars and *Bradiydius* Giesbrecht (Copepoda: Calanoida) from Southern hemisphere. *New Zealand Journal of Marine and Freshwater Research* **3(1)**:73–97 DOI 10.1080/00288330.1969.9515279.

Bradford JM. 1971. The fauna of the Ross Sea, 8: Pelagic Copepoda. *Bulletin New Zealand. Department of Scientific and Industrial Research* **206**:9–31.

Brewin RJ, Ciavatta S, Sathyendranath S, Jackson T, Tilstone G, Curran K, Airs RL, Cummings D, Brotas V, Organelli E, Dall'Olmo G, Raitsos DE. 2017. Uncertainty in ocean-color estimates of chlorophyll for phytoplankton groups. *Frontiers in Marine Science* **4**:104.

Burkov VA. 1994. Antarctic jets. *Okeanologiya* **34**:169–177.

Chapman CC, Lea MA, Meyer A, Sallée JB, Hindell M. 2020. Defining Southern Ocean fronts and their influence on biological and physical processes in a changing climate. *Nature Climate Change* **10(3)**:1–11 DOI 10.1038/s41558-020-0705-4.

Clarke KR, Warwick RM. 2001. *Changes in marine communities: an approach to statistical analysis and interpretation*. Second Edition. Plymouth: PRIMER-E.

Conroy JA, Steinberg DK, Thibodeau PS, Schofield O. 2020. Zooplankton diel vertical migration during Antarctic summer. *Deep Sea Research Part I: Oceanographic Research Papers* **162(6)**:103324 DOI 10.1016/j.dsr.2020.103324.

Constable AJ, Melbourne-Thomas J, Corney SP, Arrigo KR, Barbraud C, Barnes DKA, Bindoff NL, Boyd PW, Brandt A, Costa DP, Davidson AT, Ducklow HW, Emmerson L, Fukuchi M, Gutt J, Hindell MA, Hofmann EE, Hosie GW, Iida T, Jacob S, Johnston NM, Kawaguchi S, Kokubun N, Koubbi P, Lea M-A, Makhado A, Massom RA, Meiners K, Meredith MP, Murphy EJ, Nicol S, Reid K, Richerson K, Riddle MJ, Rintoul SR, Smith WO Jr, Southwell C, Stark JS, Sumner M, Swadling KM, Takahashi KT, Trathan PN, Welsford DC, Weimerskirch H, Westwood KJ, Wienecke BC, Wolf-Gladrow D, Wright SW, Xavier JC, Ziegler P. 2014. Climate change and Southern Ocean ecosystems I: how changes in physical habitats directly affect marine biota. *Global Change Biology* **20(10)**:3004–3025 DOI 10.1111/gcb.12623.

David PM. 1955. The distribution of *Sagitta gazellae* RitterZahony. *'Discovery' Report* **27**:235–278.

David PM. 1958. The distribution of the Chaetognatha of the Southern Ocean. *'Discovery' Report* **29**:199–228.

Deacon GER. 1937. The hydrology of the Southern Ocean. *Discovery Report* **15**:3–122.

Deacon GER. 1982. Physical and biological zonation in the Southern Ocean. *Deep-Sea Research* **29(1)**:1–15 DOI 10.1016/0198-0149(82)90058-9.

Demidov AB, Mosharov SA, Gagarin VI. 2012. Phytoplankton production characteristics in the southern Atlantic and the Atlantic sector of the Southern Ocean in the austral summer of 2009–2010. *Oceanology* **52(2)**:206–218 DOI 10.1134/S0001437012010055.

Dolzhenkov VN. 1982. *Zoogeographic zonation of the surface waters in the Pacific sector of the Southern Ocean using macroplankton in Fauna and Distribution of Temperature and Antarctic Crustaceans (Collected papers)*. Vladivostok: DVNC AN USSR Publishers, 110–116.

Foxton P. 1956. The standing crop of zooplankton in the Southern Ocean. *Discovery Report* **28**:193–235.

Fransz HG, Gonzalez SR. 1997. Latitudinal metazoan plankton zones in the Antarctic Circumpolar Current along 6oW during austral spring 1992. *Deep-Sea Research II* **44(1–2)**:395–414 DOI 10.1016/S0967-0645(96)00065-3.

Froneman PW. 2000. Feeding studies on selected zooplankton in a temperate estuary, South Africa. *Estuarine, Coastal and Shelf Science* **51(5)**:543–552 DOI 10.1006/ecss.2000.0700.

Garcia CAE, Garcia VMT, McClain CR. 2005. Evaluation of SeaWiFS chlorophyll algorithms in the Southwestern Atlantic and Southern Oceans. *Remote Sensing of Environment* **95(1)**:125–137 DOI 10.1016/j.rse.2004.12.006.

Gliwicz MZ. 1986. Predation and the evolution of vertical migration in zooplankton. *Nature* **320(6064)**:746–748 DOI 10.1038/320746a0.

Grachev DG. 1991. *Frontal zone influences on the distribution of different zooplankton groups in the central part Indian sector of the Southern Ocean in Ecology of Commercial Marine Hydrobionts (Ed. Samoilova, M.S., Shumkova).* Vladivistok: TINRO Press, 19–21.

Halfter S, Cavan EL, Swadling KM, Eriksen RS, Boyd PW. 2020. The role of zooplankton in establishing carbon export regimes in the Southern Ocean: a comparison of two representative case studies in the subantarctic region. *Frontiers in Marine Science* **7**:1–9 DOI 10.3389/fmars.2020.567917.

Hammer Ø, Harper DAT, Ryan PD. 2008. Past user manual. *Available at* http://folk.uio.no/ohammer/past/.

Hardy AC, Gunther ER. 1935. The plankton of the South Georgia whaling grounds and adjacent waters, 1926–1927. *Discovery Report* **11**:1–456.

Hopkins TL. 1971. Zooplankton standing crop in the Pacifc sector of the Antarctic. In: Llano GW, Wallen IE, eds. *Biology of the Antarctic Seas IV. Antarctic Research Series.* Vol. 4. 347–362.

Hosie GW, Mormede S, Kitchener J, Takahashi K, Raymond B. 2014. Near-surface zooplankton communities in SCAR Biogeographic Atlas of the Southern Ocean (eds. De Broyer C., Koubbi P.). Cambridge, UK: Scientific Committee on Antarctic Research, 422–430.

Jasmine P, Muraleedharan KR, Madhu NV, Ashadevi CR, Alagarsamy R, Achuthankutty CT, Revi ZP, Sanjeevan VN, Sahayak S. 2009. Hydrographic and biological characteristics along 45 E longitude in the South Western Indian Ocean and Southern Ocean during austral summer 2004. *Marine Ecology Progress Series* **389**:97–116 DOI 10.3354/meps08126.

Kulagin DN. 2010. Distribution of chaetognaths in the central part of the Drake Passage. *Oceanology* **50(4)**:513–521 DOI 10.1134/S0001437010040077.

Labat JP, Mayzaud P, Dallot S, Errhif A, Razouls S, Sabini S. 2002. Mesoscale distribution of zooplankton in the sub-antarctic frontal system in the Indian part of the Southern Ocean: a comparison between optical plankton counter and net sampling. *Deep Sea Research Part I: Oceanographic Research Papers* **49(4)**:735–749 DOI 10.1016/S0967-0637(01)00076-0.

Labat JP, Gasparini S, Mousseau L, Prieur L, Boutoute M, Mayzaud P. 2009. Mesoscale distribution of zooplankton biomass in the northeast Atlantic Ocean determined with an optical plankton counter: relationships with environmental structures. *Deep Sea Research Part I: Oceanographic Research Papers* **56(10)**:1742–1756 DOI 10.1016/j.dsr.2009.05.013.

Lampert W. 1989. The adaptive significance of diel vertical migration of zooplankton. *Functional Ecology* **3(1)**:21–27 DOI 10.2307/2389671.

Lebourges-Dhaussy A, Coetzee J, Hutchings L, Roudaut G, Nieuwenhuys C. 2009. Zooplankton spatial distribution along the South African coast studied by multifrequency acoustics, and its

relationships with environmental parameters and anchovy distribution. *ICES Journal of Marine Science* **66(6)**:1055–1062 DOI 10.1093/icesjms/fsp129.

Legendre P, Legendre L. 1998. *Numerical ecology.* Amsterdam, Netherlands: Elsevier.

Lomakina NB. 1964. *Fauna Euphausiacea of the Antarctic and notal areas in The results of biological research of the Soviet Antarctic Expedition (1955–1958).* Vol. 2. Moscow: Nauka, 254–334 [In Russian].

Longhurst AR. 1976. Interactions between zooplankton and phytoplankton profiles in the eastern tropical Pacific Ocean. *Deep Sea Research and Oceanographic Abstracts* **23(8)**:729–754 DOI 10.1016/S0011-7471(76)80017-4.

Lucas CH, Jones DOB, Hollyhead CJ, Condon RH, Duarte CM, Graham WM, Robinson KL, Pitt KA, Schildhauer M, Regetz J. 2014. Gelatinous zooplankton biomass in the global oceans: geographic variation and environmental drivers. *Global Ecology and Biogeography* **23(7)**:701–714 DOI 10.1111/geb.12169.

Lumpkin R, Speer K. 2007. Global ocean meridional overturning. *Journal of Physical Oceanography* **37(10)**:2550–2562 DOI 10.1175/JPO3130.1.

Mackintosh NA. 1934. Distribution of the macroplankton in the Atlantic sector of the Antarctic. *Discovery Report* **16**:365–412.

Mackintosh NA. 1937. The seasonal circulation of the Antarctic macroplankton. *Discovery Report* **16**:365–412.

Mayewski PA, Meredith MP, Summerhayes CP, Turner J, Worby A, Barrett PJ, van Ommen T. 2009. State of the Antarctic and Southern Ocean climate system. *Reviews of Geophysics* **47(1)**:RG1003 DOI 10.1029/2007RG000231.

McGinnis RF. 1977. *Evolution within pelagic ecosystems: aspects of the distribution and evolution of the family Myctophidae. Adaptations within Antarctic Ecosystems.* Washington, DC: Smithsonian Institution, 547–556.

Nowlin WD Jr, Clifford M. 1982. The kinematic and thermohaline zonation of the Antarctic Circumpolar Current at Drake Passage. *Journal of Marine Research* **40**:481–507.

Ommanney FD. 1936. *Rhincalanus gigas* (Brady) a copepod of the southern macroplankton. *Discovery Report* **13**:277–384.

Orsi H, Whitworth T III, Nowlin WD Jr. 1995. On the meridional extent and fronts of the Antarctic Circumpolar Current. *Deep Sea Research Part I: Oceanographic Research Papers* **42**:641–673.

Pakhomov EA, Froneman P, Shreeve R, Atkinson A, Korb B, Whitehouse M, Thorpe S, Pond D, Cunningham N. 2006. Plankton community structure and variability in the Scotia Sea: austral summer 2003. *Marine Ecology Progress Series* **309**:75–91 DOI 10.3354/meps309075.

Pakhomov EA, Froneman PW. 2004a. Zooplankton dynamics in the eastern Atlantic sector of the Southern Ocean during the austral summer 1997/1998—part 1: community structure. *Deep Sea Research Part II: Topical Studies in Oceanography* **51**:2599–2616.

Pakhomov EA, Froneman PW. 2004b. Zooplankton dynamics in the eastern Atlantic sector of the Southern Ocean during the austral summer 1997/1998—part 2: grazing impact. *Deep Sea Research Part II: Topical Studies in Oceanography* **51**:2617–2631.

Pakhomov EA, Perissinotto R, McQuaid CD. 1994. Comparative structure of the macrozooplankton/micronekton communities of the Subtropical and Antarctic Polar Fronts. *Marine Ecology Progress Series* **111(1)**:155–169 DOI 10.3354/meps111155.

Pakhomov EA, McQuaid CD. 1996. Distribution of surface zooplankton and seabirds across the Southern Ocean. *Polar Biology* **16(4)**:271–286 DOI 10.1007/s003000050054.

Pakhomov EA, Perissinotto R, McQuaid CD, Froneman PW. 2000. Zooplankton structure and grazing in the Atlantic sector of the Southern Ocean in late austral summer 1993: part 1. Ecological zonation. *Deep Sea Research Part I: Oceanographic Research Papers* **47(9)**:1663–1686 DOI 10.1016/S0967-0637(99)00122-3.

Park ET, Ferrari FD. 2009. *pecies diversity and distributions of pelagic calanoid copepods (Crustacea) from the Southern Ocean in Smithsonian at the poles: contributions to international polar year science (ed. Krupnik I., et al.).* Washington, D.C., USA: Smithsonian Institution Scholarly Press, 143–179.

Pinkerton MH, Bradford-Grieve JM. 2014. Characterizing foodweb structure to identify potential ecosystem effects of fishing in the Ross Sea, Antarctica. *ICES Journal of Marine Science* **71(7)**:1542–1553 DOI 10.1093/icesjms/fst230.

Pinkerton MH, Smith ANH, Raymond B, Hosie GW, Pollard RT, Bathmann U, Dubischar C, Read JF, Lucas M. 2002. Zooplankton distribution and behaviour in the Southern Ocean from surveys with a towed Optical Plankton Counter. *Deep Sea Research Part II: Topical Studies in Oceanography* **49(18)**:3889–3915 DOI 10.1016/S0967-0645(02)00116-9.

Rudjakov YA, Voronina NM. 1973. Daily vertical migration of copepods *Metridia gerlachei* in the Scotia Sea. *Oceanology* **13**:512–514.

Smetacek V, Klaas C, Menden-Deuer S, Rynearson TA. 2002. Mesoscale distribution of dominant diatom species relative to the hydrographical field along the Antarctic Polar Front. *Deep Sea Research Part II: Topical Studies in Oceanography* **49(18)**:3835–3848 DOI 10.1016/S0967-0645(02)00113-3.

Sokolov S, Rintoul SR. 2009. Circumpolar structure and distribution of the Antarctic Circumpolar Current fronts: 2. Variability and relationship to sea surface height. *Journal of Geophysical Research: Oceans* **114(C11)**:8081 DOI 10.1029/2008JC005248.

Steinberg DK, Landry MR. 2017. Zooplankton and the ocean carbon cycle. *Annual Review of Marine Science* **9(1)**:413–444 DOI 10.1146/annurev-marine-010814-015924.

Steinberg DK, Ruck KE, Gleiber MR, Garzio LM, Cope JS, Bernard KS, Stammerjohn SE, Schofield OME, Quetin LB, Ross RM. 2015. Long-term (1993–2013) changes in macrozooplankton off the western antarctic peninsula. *Deep Sea Research Part I: Oceanographic Research Papers* **101(2)**:54–70 DOI 10.1016/j.dsr.2015.02.009.

Stupnikova AN, Vereshchaka AL. 2013. High-resolution survey indicates high heterogeneity in copepod distribution in the hydrologically active Drake Passage. *Journal of Natural History* **47(5–12)**:699–713 DOI 10.1080/00222933.2012.708451.

Stupnikova AN, Tarakanov RY, Kulagin DN, Vereshchaka AL. 2018. Factors maintaining the identity of mesoplankton communities: cool evidence from the Drake Passage. *Hydrobiologia* **809(1)**:221–232 DOI 10.1007/s10750-017-3474-y.

Takahashi KT, Hosie GW, Kitchener JA, McLeod DJ, Odate T, Fukuchi M. 2010. Comparison of zooplankton distribution patterns between four seasons in the Indian Ocean sector of the Southern Ocean. *Polar Science* **4(2)**:317–331 DOI 10.1016/j.polar.2010.05.002.

Takahashi KT, Kawaguchi S, Kobayashi M, Hosie GW, Fukuchi M, Toda T. 2002. Zooplankton distribution patterns in relation to the Antarctic Polar Front Zones recorded by Continuous Plankton Recorder (CPR) during 1999-2000 Kaiyo Maru cruise. *Polar Bioscience* **15**:97–107.

Tarakanov RY, Gritsenko AM. 2014. Fine-jet structure of the Antarctic Circumpolar Current south of Africa. *Oceanology* **54(6)**:677–687 DOI 10.1134/S0001437014050130.

Ter Braak CJ. 1986. Canonical correspondence analysis: a new eigenvector technique for multivariate direct gradient analysis. *Ecology* **67(5)**:1167–1179 DOI 10.2307/1938672.

Thibodeau PS, Steinberg DK, Stammerjohn SE, Hauri C. 2019. Environmental controls on pteropod biogeography along the Western Antarctic Peninsula. *Limnology and Oceanography* **64(S1)**:240–256 DOI 10.1002/lno.11041.

Vedenin AA, Kulagin DN, Musaeva EI, Vereshchaka AL. 2020. The Southern Polar Front as a key to mesoplankton migratory behavior. *Scientific Reports* **10(1)**:1–14 DOI 10.1038/s41598-020-70720-9.

Vedenin AA, Musaeva EI, Zasko DN, Vereshchaka AL. 2019. Zooplankton communities in the Drake Passage through environmental boundaries: a snapshot of 2010, early spring. *PeerJ* **e7994(2–3)**:7994 DOI 10.7717/peerj.7994.

Vereshchaka A, Abyzova G, Lunina A, Musaeva E, Sutton T. 2016. A novel approach reveals high zooplankton standing stock deep in the sea. *Biogeosciences* **13(22)**:6261–6271 DOI 10.5194/bg-13-6261-2016.

Vereshchaka A, Abyzova G, Lunina A, Musaeva E. 2017. The deep-sea zooplankton of the North, Central, and South Atlantic: biomass, abundance, diversity. *Deep Sea Research Part II: Topical Studies in Oceanography* **137**:89–101 DOI 10.1016/j.dsr2.2016.06.017.

Vereshchaka AL, Lunina AA, Sutton T. 2019. Assessing deep-pelagic shrimp biomass to 3000 m in the Atlantic Ocean and ramifications of upscaled global biomass. *Scientific Reports* **9(1)**:5946 DOI 10.1038/s41598-019-42472-8.

Vervoort W. 1965. Notes on the biography and ecology of freeliving marine copepoda. *Biogeography and Ecology in Antarctica* **15**:381–400.

Vinogradov ME, Shushkina EA, Vereshchaka AL, Nezlin NP. 1996. On migrations of *Calanus finmarchicus* sl in the Norwegian Sea during the polar day. *Oceanology of the Russian Academy of Sciences* **36**:59–63.

Voronina NM. 1984. Ecosystems of pelagial of the Southern Ocean. *Nauka Moscow* **1**:206.

Ward P, Whitehouse M, Brandon M, Shreeve R, Woodd-Walker R. 2003. Mesozooplankton community structure across the Antarctic Circumpolar Current to the north of South Georgia: southern ocean. *Marine Biology* **143(1)**:121–130 DOI 10.1007/s00227-003-1019-6.

Ward PJ, Jongman B, Kummu M, Dettinger MD, Weiland FCS, Winsemius HC. 2014. Strong influence of El Niño Southern Oscillation on flood risk around the world. *Proceedings of the National Academy of Sciences of the United States of America* **111(44)**:15659–15664 DOI 10.1073/pnas.1409822111.

Zeng C, Xu H, Fischer A. 2016. Chlorophyll-a estimation around the Antarctica peninsula using satellite algorithms: hints from field water leaving reflectance. *Sensors* **16(12)**:2075 DOI 10.3390/s16122075.

Żmijevska MI. 1987. Horizontal and vertical distribution of Copepoda in the Southern part of the Drake Passage and in the Bransfield Strait. BIOMASS-SIBEX. *Polish Polar Research* **8**:381–390.